

Efficiency measurements at Vessingfoss power station

Leif Ragnar Rundquist Parr

Master of Science in Energy and Environment
Submission date: June 2007
Supervisor: Ole Gunnar Dahlhaug, EPT

Problem Description

1. The student shall plan, design and aid in producing the equipment necessary to carry out efficiency measurements at Vessingfoss power station.
2. The student shall measure hydraulic turbine efficiency by the thermodynamic method at Vessingfoss power station.
3. The student shall use the results to consider possible measures to improve the power station.
4. If there is time, the student shall carry out measurements at another power station.

Assignment given: 01. February 2007
Supervisor: Ole Gunnar Dahlhaug, EPT

Abstract

A measurement of the hydraulic turbine efficiency at the Vessingfoss hydro power station by the thermodynamic method has been attempted, but has not given the desired results.

Two problems have been encountered. The high pressure side temperature measurements show an abnormal scatter resulting in standard deviations of $s_y=0.05^\circ\text{C}$. The reason for the scatter may be temperature layers in the reservoir lake Nesjø. This theory has been investigated, but needs further work.

The other problem has been the mechanical strength of the low pressure side collector probes. Two different collectors have been tried, and both have broken down. The second attempt was made with a collector design based on wire rope, which failed because the turnbuckles were under-dimensioned. With proper dimensions, this solution is interesting in the future, as it was easy to install and may contribute to lose collector weight.

The relative turbine efficiency has been calculated based on pressures and levels measured during the thermodynamic test. An uncertainty analysis of the result has been carried out. The head loss has been calculated based on technical drawings of the penstock and loss coefficients from the literature.

Acknowledgements

The master thesis has been performed at the Waterpower Laboratory at the Norwegian University of Science and Technology, and at the Vessingfoss power station in Tydal. I express my sincere thanks to my supervisor Ole Gunnar Dahlhaug who initiated this work, and to PhD-student Håkon Hjort Francke, who assisted on the field experiment, for invaluable tutoring and support. I wish to thank Joar Grilstad at the Waterpower Laboratory, who has helped with practical details regarding the instrumentation.

Trondheim Energy in Tydal have been very co-operative, of whom Kjell Olav Gresli, Gisle Kjøsnes and Per Horven deserve a special thanks.

Trondheim, June 2007

Contents

1	The Vessingfoss power station	1
2	Experimental setup and equations.....	3
2.1	The thermodynamic method.....	3
2.2	Expected temperature difference.....	4
2.3	High pressure side probe	4
2.4	High pressure side cross-section area.....	5
2.5	The low pressure side collector probe.....	5
2.5.1	Design methods for draft tube probe collectors	7
2.5.2	Fall 2006: Dimensioning of pipes	8
2.5.3	Spring 2007: Dimensioning of turnbuckles	9
2.6	LPS Collector probe flow.....	10
2.7	Generator efficiency	10
2.8	Generator power	11
2.9	Leakage water flow	12
2.10	Index measurement setup and equations	13
2.11	Uncertainty	14
2.12	Head loss	15
2.13	Calibration.....	16
3	Results	17
3.1	Thermodynamic method	17
3.1.1	The LPS collector flow experiment	18
3.2	Index measurement	19
3.3	Uncertainty in the relative turbine efficiency.....	20
3.4	Turbine efficiency with theoretic head loss	21

4	Discussion	22
4.1	The thermodynamic method.....	22
4.1.1	HPS temperature scatter	22
4.1.2	Draft tube collector probes-fall 2006.	23
4.1.3	Draft tube collector probes-spring 2007.....	24
4.2	Index measurement	25
4.2.1	Efficiency with head loss	25
4.2.2	Rejection of outliers	25
4.3	Uncertainty	25
4.3.1	Random uncertainty	26
4.3.2	Systematic uncertainty	26
4.4	Observations at Vessingfoss.....	27
4.4.1	kWh-counter and measurement transformers	27
4.4.2	Gas bubbles in the leakage water	28
4.4.3	Draft tube surge tank and cavitation	28
5	Further work	29
5.1	Further measurements at Vessingfoss: Gibson's method	29
5.2	Installation of Winter-Kennedy pressure tapings.....	29
6	Conclusion.....	30
	Bibliography.....	31
	Appendix.....	33

List of tables

Table 1-1: <i>Vessingfoss turbine data</i>	1
Table 2-1: <i>Points and loads for April 2007 measurement at Vessingfoss.</i>	3
Table 2-2: <i>Estimate of the HPS cross-section area based on 2x3 measured diameters.</i>	5
Table 2-3: <i>Simulated efficiencies for the generator at Vessingfoss.</i>	10
Table 2-4: <i>Calibration of instruments.</i>	16
Table 3-1: <i>Calculation and results of uncertainty analysis of the relative turbine efficiency.</i>	20
Table 4-1: <i>Input and results from design of Vessingfoss LPS collector probes.</i>	24
Table 4-2: <i>Comparison of index test BEP with analytic BEP from Statkraft Grøner.</i>	25

List of figures

Figure 2-1: <i>Instrument setup for the thermodynamic test at Vessingfoss.</i>	3
Figure 2-2: <i>HPS Probe for measurement of temperature and pressure. (Francke and Wiborg, 2005 p22)</i>	4
Figure 2-3: <i>Overview of the LPS collector probe used in the fall 2006 measurement. Detail: Wall bracket and collector pipe. NB! The clamps between the pipe and bracket are not shown.</i>	5
Figure 2-4: <i>Overview of the LPS collector probe used in the spring 2007 measurement. Details: Left - Pipe with channel bar for wire rope guidance. Right - Turnbuckle and wall t-piece.</i>	6
Figure 2-5: <i>Collector probe area subject to flow drag, orthogonal to the main flow direction.</i>	8
Figure 2-6: <i>Schematic diagram of collector pipe looking into the vertical plane.</i>	8
Figure 2-7: <i>Model of wire rope based LPS collector probe.</i>	9
Figure 2-8: <i>Draft tube collector flow measurement setup.</i>	10
Figure 2-9: <i>Power measurement connection points (excerpt from TEV drawings). g51 is the station kWh- counter.</i>	11
Figure 2-10: <i>Overview of index measurement parameters at Vessingfoss.</i>	13
Figure 3-1: <i>HPS temperature scatter at Vessingfoss.</i>	18
Figure 4-1: <i>Flow separation at the inner wall of a 90 degree bend with $Re_d \geq 0.3 \times 10^6$. (Idelchik, 1994)</i>	22
Figure 4-2: <i>Section view of Vessingfoss turbine from general technical drawing.</i>	28
Figure 5-1: <i>Location of taps for the Winter-Kennedy method of discharge measurement through a turbine equipped with a steel spiral case (IEC, 1991 figure 66).</i>	29

Abbreviations

LPS. The low pressure side of the turbine.

HPS. The high pressure side of the turbine.

IEC. The international electrotechnical commission.

TEV. Trondheim Energiverk, which changed name in 2007 to Trondheim Energy.

BEP. Best efficiency point - the state at which a turbine attains its highest efficiency.

PSPP. Pumped storage power station, a hydro power station which can pump and generate.

IGHM. The international group for hydraulic efficiency measurement.

CFD. Computational fluid dynamics. Numerical finite element methods in fluid dynamics.

LDV. Laser Doppler velocimeter. An experimental technique using the Doppler shift of laser light to determine velocities (Dahlhaug, 1997 p16).

PIV. Particle image velocimetry. A technique of measuring the velocity vectors within a flow by taking optical photos of the movement of small particles added to the flow (Prasad, 2000).

RMS. Root mean square. $a = \sqrt{b^2 + c^2}$

Nomenclature and indices

Symbol	Description	Unit
$\phi = \frac{\rho q}{\rho_1 Q_1}$	Ratio of the mass flow of leakage water to the HPS mass flow.	-
$\varphi = \frac{Q}{Q_{BEP}}$	Relative flow rate.	-
$\rho = f(p, T)$	Specific weight of water	kg/m ³
η_m	Mechanical turbine efficiency	%
η_h	Hydraulic turbine efficiency	%
η_g	Generator efficiency	%
$\eta = \eta_m \eta_h$	Turbine efficiency	%
η^*	Relative turbine efficiency, with the highest efficiency value set to 100%	%
A	Cross-section area	m ²
FR	Flow repartition, the percentage of the flow passing through the channel of interest.	%
H_0	Rated head	m
g	Gravity	m/s ²
k	Head loss constant, $h=kQ^2$	s ² /m ⁵
n	Number of data points in a sample.	
$n_q = \frac{n\sqrt{Q_0}}{H_0^{3/4}}$	Metric specific speed as defined by Gordon (2001)	$\frac{rpm \times m^{3/4}}{\sqrt{s}}$
M	Resultant moment in point P	Nm
P	Turbine power, i.e the power delivered to the generator through the shaft, after all mechanical losses have been accounted for	W
P_a	Generator power	W
p	Pressure	kPa
p_{IP}	HPS ring pressure measured on the turbine floor	kPa
Δp	Pressure correction from calibration verification of Digiquartz transducers	kPa
Q	Flow	m ³ /s
Q_0	Nominal flow.	m ³ /s
S	Swirl number, the flux of angular momentum divided by the flux of axial momentum.	-
s_y	The sample standard deviation	
t	Coefficient of the student's T-distribution, or time	s
V	Resultant force in point P	N
v	Velocity	m/s
z	Altitude (meters above sea level)	m.a.s.
Δz	The height between a threshold of known altitude and the tailwater level	m
$1, 1-1$	HPS, in the centreline of the pipe directly upstream of the spiral casing. In the HPS probe.	
$2, 2-1, 2-2$	LPS, in the centreline of the draft tube right upstream of the draft tube gates. The LPS collector frames	
3	The leakage water from the upper labyrinth seal	
p	Turbine floor	

1 The Vessingfoss power station

The Vessingfoss power station is situated between the Nesjø and Vessingsjø reservoirs in Tydal. The plant was commissioned in 1971. Since then, no field efficiency measurements have been made to establish turbine performance, except for a poorly documented index test in 1975. The low head Francis turbine runs very rough on part load, with a great deal of vibrations and pressure pulsations. In addition, there is cavitation, which has to be repaired every fourth or fifth year. Today, Trondheim Energy (TEV) only operates the turbine in a limited area around the best efficiency point (BEP).

Table 1-1: Vessingfoss turbine data

Year of commissioning	1971
Turbine manufacturer	Kværner Brug A/S
Turbine type	Francis
Rated head	55m
Rated output	40MW
Rated flow	85m ³ /s
Rotational speed	214 rpm
Specific speed	$97.7 \text{ rpm} \times \text{m}^{3/4} / \sqrt{s}$

The problems at Vessingfoss mentioned above indicate that there is potential for improvement. Gathering accurate data on turbine performance is one essential step in making plans for upgrading the power station.

There are several methods for measuring the efficiency of a hydro power turbine in the field. The choice of methods is related to uncertainty, cost and complexity. Svean power station is another TEV-operated low head Francis turbine. Francke and Wiborg (2005) demonstrated that the thermodynamic method can be used at heads down to 50m, and that the uncertainty at this head is on the same order of magnitude as the uncertainty of Gibson's method. However, Gibson's method is difficult and costly when there is no external access to the penstock, as is the case at Vessingfoss (Adamkowski et. al, 2006). The thermodynamic method is less costly and time consuming in installation, and was therefore chosen for measurements at Vessingfoss.

There is also an academic side to this choice. Turbine efficiency measurements are regulated by the international standard IEC 60041, which is widely used to determine if contract guarantees between turbine producers and station owners are fulfilled. The standard states that the thermodynamic method only can be used for heads above 100m (IEC 60041, 1991 p293). If there is to be a revision of the standard, it is important to have sufficient amounts of data on low head thermodynamic measurements, so the 100m limit can be thoroughly discussed. Measuring by the thermodynamic method at Vessingfoss contributes to this end.

Another objective of the measurement is to quantify the flow through the low pressure side collector probe used in the thermodynamic test. The long term objective of such work is to investigate the possibility of scaling down the collector pipe structure, to limit weight and make installation easier. Such a possibility is interesting in the case where the collector pipe function primarily is to sample water, and there is another element that takes up the stress, like wire rope. This was attempted by installing a pitot-static tube in the collector outlet pipe.

In March 2007, the author assisted a thermodynamic hydraulic efficiency acceptance test of two pump-turbines in the Cheongsong pumped storage power station, Korea. Considerations from this test situation will be used to shed light on some aspects of the Vessingfoss test.

2 Experimental setup and equations

2.1 The thermodynamic method

For a general introduction to the thermodynamic method, see for example Kjølle (2003). Disregarding the low Vessingfoss head, the thermodynamic test was carried out in accordance with the IEC 60041:1991 standard. The instruments were set up according to figure 2-1 below.

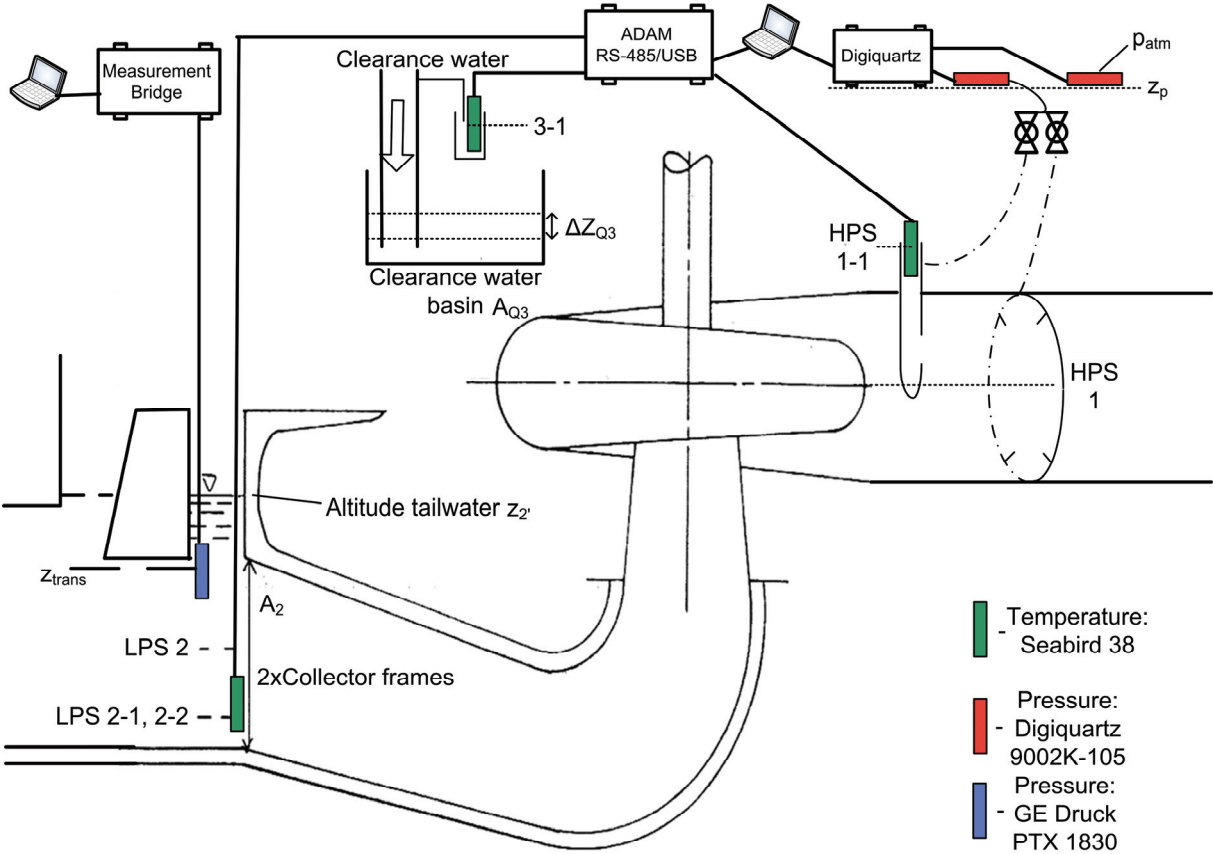


Figure 2-1: Instrument setup for the thermodynamic test at Vessingfoss.

The choice of points was based on two considerations. Firstly, there exist certain limits to the operation range of the Vessingfoss turbine, as described in the introduction. The use of data outside of the operating range is of limited interest to TEV. Secondly, it was important to record several runs with the unit in the same state to allow a direct evaluation of the random uncertainty of the turbine efficiency and turbine power through statistical analysis. This was done towards the end of the test, in points 11 through 13. The chosen measurement point generator loads are shown in table 2-1 below.

Table 2-1: Points and loads for April 2007 measurement at Vessingfoss.

Point	1	2	3	4	5	6	7	8	9	10	11	12	13
Generator load[MW]	36	33.6	18.8	37.2	39.2	40	38.4	37.2	36.4	34.8	38	38	38

2.2 Expected temperature difference

It is important to know beforehand that the thermometers are capable of accurately recording the expected temperature difference over the turbine. Therefore, the difference must be estimated or compared to similar sites. Kjølle (2003 p119) presents a simplified method of approximating the temperature difference over the turbine. At net head $H=52\text{m}$, assuming a hydraulic efficiency of $\eta_h=90\%$, the method gives:

$$\Delta T = \frac{(1-\eta_h)Hg}{C_p} = 0.012^\circ\text{C} \quad (1)$$

At Svean (Francke and Wiborg, 2005), the measured temperature difference over turbine one was $\Delta T=0.011^\circ\text{C}$ for a hydraulic efficiency of $\eta_h=89.8\%$ and effective head $H=52.6\text{m}$, which is in agreement with Kjølle.

2.3 High pressure side probe

A probe was set up to measure the specific energy at the turbine inlet (see figure 2-2). This is done by measuring temperature, probe pressure and probe flow. At Vessingfoss, the high pressure side (HPS) diameter is 3.8m. IEC (1991) suggests the use of two HPS probes for diameters between 2.5 and 5m. Most of the inlet pipe and spiral casing is cast-in, and consequently it was only possible to install one HPS probe.

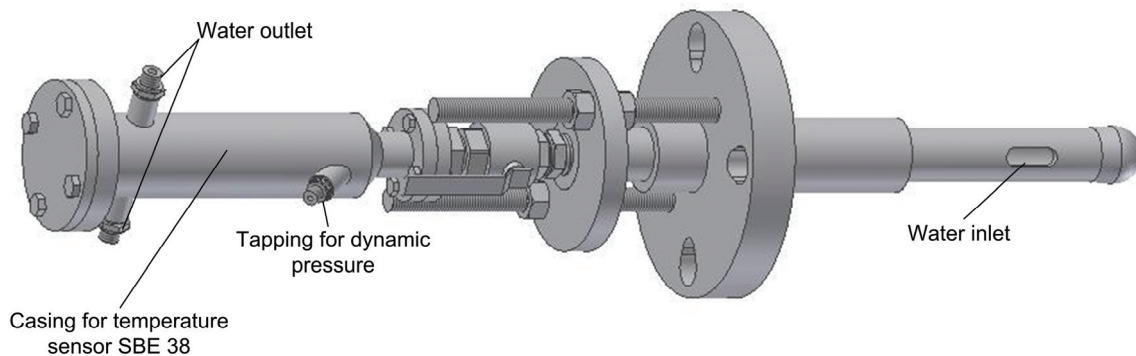


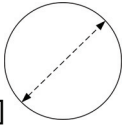
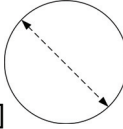
Figure 2-2: HPS Probe for measurement of temperature and pressure. (Francke and Wiborg, 2005 p22)

Since the Waterpower Laboratory does not possess a calibrated rotameter, the probe flow was derived from the time the flow used to fill a bucket. This is more tedious than using a rotameter, but both methods suffice as limited accuracy is needed. A stop watch and a bucket of known volume were used for this purpose.

2.4 High pressure side cross-section area

The HPS cross-section area A_1 was measured upon inspection inside the spiral casing. A laser distance meter was used for finding 2 orthogonal diameters, each based on three measurements (see the table 2-2 below). The area is calculated from the average diameter of all six measurements.

Table 2-2: Estimate of the HPS cross-section area based on 2x3 measured diameters.

 D_1 [m]	3.806	 D_2 [m]	3.880
	3.808		3.882
	3.809		3.881
Average D [m]	3.844		
Area A_1 [m ²]	11.607		

2.5 The low pressure side collector probe

Making use of a collector probe is a way of sampling the water temperature over the whole draft tube cross-section using only one thermometer. The method is validated by Dahlhaug and Brekke (1996). The low pressure side (LPS) measuring section at Vessingfoss is set directly upstream from the draft tube gates. At this point, the draft tube is split in two channels by a pier, which means that two collectors and two thermometers are needed. This is done because a collector which would span the whole 7.5m width upstream of the pier would need an enormous support structure to resist flexion. In addition, it is convenient to stretch the temperature cables through two aeration holes located right upstream of the draft tube gates.

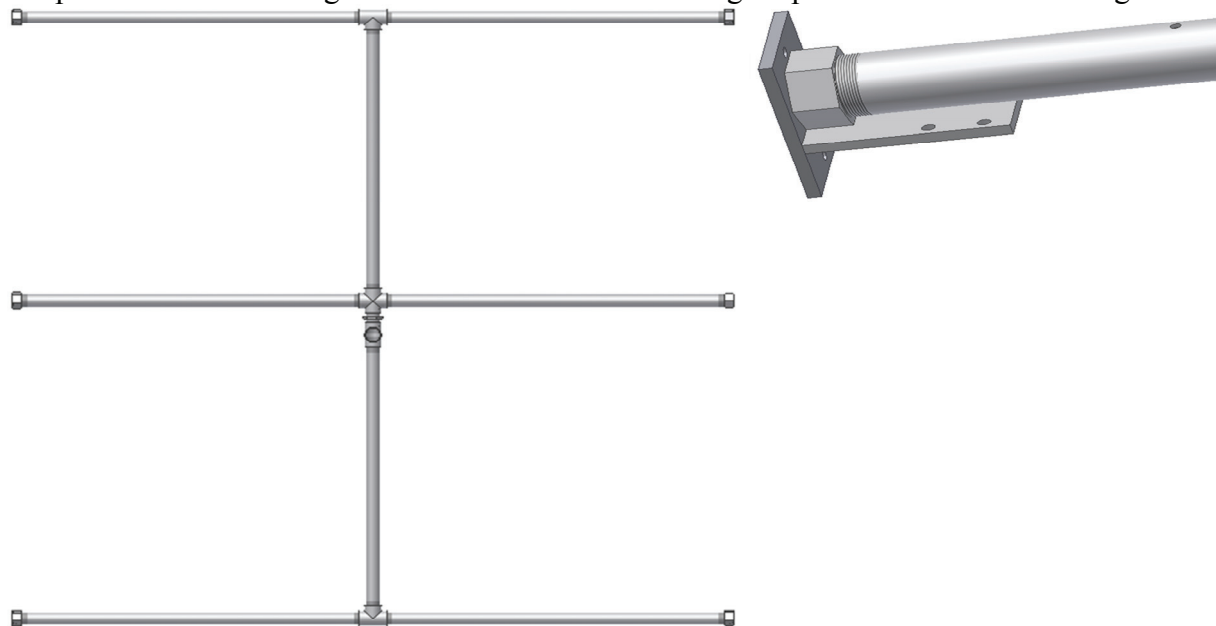


Figure 2-3: Overview of the LPS collector probe used in the fall 2006 measurement. Detail: Wall bracket and collector pipe. NB! The clamps between the pipe and bracket are not shown.

The design of the first draft tube collector probe (see figure 2-3) was based on the design used with success at Svean (Francke and Wiborg, 2005 appM-N). The pipe length was modified to fit the Vessingfoss draft tube width, and the number of horizontal pipes was increased from two to three. At Vessingfoss, the draft tube gate guides are one-sided, so that it is impossible to use them keep the collector probe in place, contrary to at Svean. Therefore, the collector

probe was fastened to the draft tube wall with wall brackets. A total of 12 expansion bolts were used to fasten the six wall brackets to the concrete wall. No calculation of mechanical strength was made of the new collector design prior to the thermodynamic test scheduled for October 2006. The draft tube collector probes and the inlet probe were installed in September, one month before the test was to take place. This was due to the plant operating scheme at the time.

The April 2007 collector probe design was based on wire rope (see figure 2-4). The concept was made up at the Waterpower Laboratory, and TEV was responsible for the detailed design and dimensioning of the parts. The idea of the design was that the wire ropes should take up and transfer the flow drag force to the wall, limiting the stress on the collector pipes themselves. In addition, the wire rope allows for some movement along the axis of the draft tube, which may increase the resistance to dynamic stress. Channel bars were welded to the collector pipes to fix the pipes to the wire ropes in the vertical plane. The wire ropes were tightened with 12mm turnbuckles, one per horizontal pipe. In addition, a wire rope was fastened between a bracket in the draft tube floor upstream of the collector probe and the middle of the collector probe. This wire rope was tightened with 16mm turnbuckles that were found in the TEV workshop as a last-minute solution.

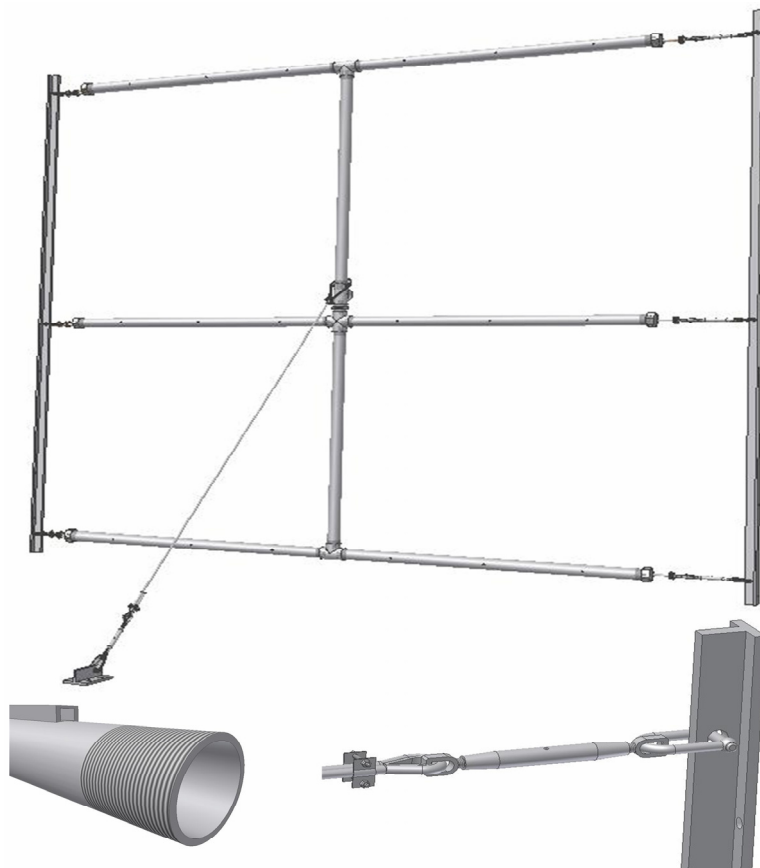


Figure 2-4: Overview of the LPS collector probe used in the spring 2007 measurement. Details: Left - Pipe with channel bar for wire rope guidance. Right - Turnbuckle and wall t-piece.

The wall brackets of the fall 2006 collector were replaced with vertical t-pieces. The t-pieces were attached to the wall with 10 expansion bolts per piece, which means that the total number of bolts per collector increased from 12 to 20. There was no plant operation between installation the 17.04 and 18.04, and operation the 19.04 and 20.04.

2.5.1 Design methods for draft tube probe collectors

The design of a draft tube collector probe must take into consideration the following factors: Mechanical strength, adequate flow through the collector probe, arrangement for the temperature cables to reach the recording unit, and installation time and difficulty.

Practice varies in the design of draft tube probe collectors, and little is found in literature. One common method is simply to modify a successful design from a test at a similar power station. This was done in the acceptance test at the Cheongsong power station, and also on the fall 2006 Vessingfoss collector. Both examples show that this method is not without risk. The Vessingfoss example is obvious, as modifying the Svean collector ended in a total breakdown.

In Cheongsong, the collector and support structure design inherited from a test at a Chinese power station worked fine. However, the shoes fastening the structure to the draft tube pipe wall were bent due to strong rotation in the flow. This had to be improved on site by welding support pieces onto the shoes. In addition, there were problems protecting the thermometer cable, which resulted in the loss of several thermometers. In total, one week was spent on improvement of the draft tube collector probe before the first successful measurement could be made. This week represents expenses in station down-time and in project hours for the measurement team, which possibly could have been saved by making a greater pre-test effort at evaluating the collector stress.

No dimensioning calculations were done for the Vessingfoss collectors beforehand. But it is nevertheless of interest to develop simple models to evaluate the collector stress and compare them with what actually happened at Vessingfoss. Two models are developed below, one for a pipe structure solution, and one for a wire rope solution. A problem with both models is evaluating the load. The turbine operating at full load presents the most severe load on the collector probes, because the flow is greatest. In addition, there is swirl flow introduced by the turbine at off design operation, which at full load rotates in the opposite direction of the runner (Vekve, 2004 p3). Iliescu, Ciocan and Avellan (2002) have carried out an experimental investigation on model of a Francis turbine draft tube with one pier. The investigation is carried out for relative flow rates of $\varphi \in [0.3; 0.4]$, i.e. at part load. Their results show that the repartition of flow (FR) between the two channels is unevenly distributed. For a relative flow rate of $\varphi=0.3$, 72% of the flow passes through the left channel. This is due to a longitudinal vortex which reduces the effective flow area of the right channel. Even though these results do not apply directly to full load operation, they are valuable in that they introduce the notion of the unevenly distributed flow repartition. This leads to higher velocities and thus higher strain on one of the collector probes. The problem still remains, however, that there is no knowledge of the station conditions a priori, except the main characteristics. Assumptions of draft tube outlet swirl S , flow repartition between channels and the effect of swirl flow on drag must be made. In the following, the swirl effects are approximated by introducing a swirl-equivalent velocity which is of equal magnitude and direction as the mean flow velocity. The dimensioning velocity is then:

$$v_{\text{dim}} = v_{\text{mean}} \frac{2FR}{100} (1+S) \left[\frac{m}{s} \right] \quad (2)$$

2.5.2 Fall 2006: Dimensioning of pipes

The collector probe is modelled as one horizontal pipe. The maximum load on this pipe is the flow drag due to the dimensioning velocity orthogonal to the collector frontal area shown in figure 2-5. It is assumed that each horizontal pipe bears exactly one third of the total probe load, since there are three horizontal pipes.

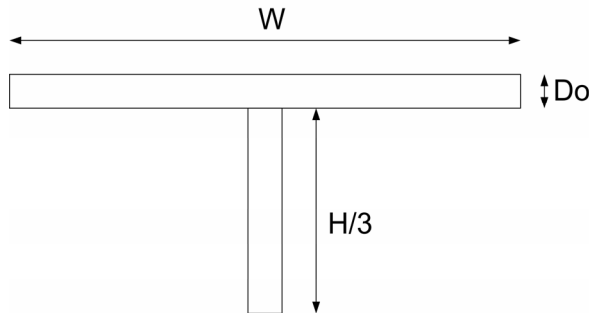


Figure 2-5: Collector probe area subject to flow drag, orthogonal to the main flow direction.

As a worst-case scenario, the drag is calculated by assuming that the pipes experience the full stagnation pressure of the uniform velocity, in other words a drag coefficient $C_D=1$. This assumption gives an extra safety margin, as the real drag coefficient is more likely to be $C_D=0.3$ (White, 1999 p458). The basis for the dimensioning is a mean flow velocity of 3 m/s, which equals a flow of $Q_2=104 \text{ m}^3/\text{s}$. As the flow of Vessingfoss is not likely to exceed $95 \text{ m}^3/\text{s}$, the above assumption takes into account the eventuality of a small unbalance in the flow distribution between the two channels. Adding the swirl-equivalent velocity, a dimensioning velocity of 6m/s is derived. The weight of the collector itself is small compared to the drag force, and is neglected.

The drag force from the vertical pipe section is modelled by a force F acting on the middle of the horizontal pipe. The drag on the horizontal pipe is modelled as a force per length q equally distributed along the pipes.

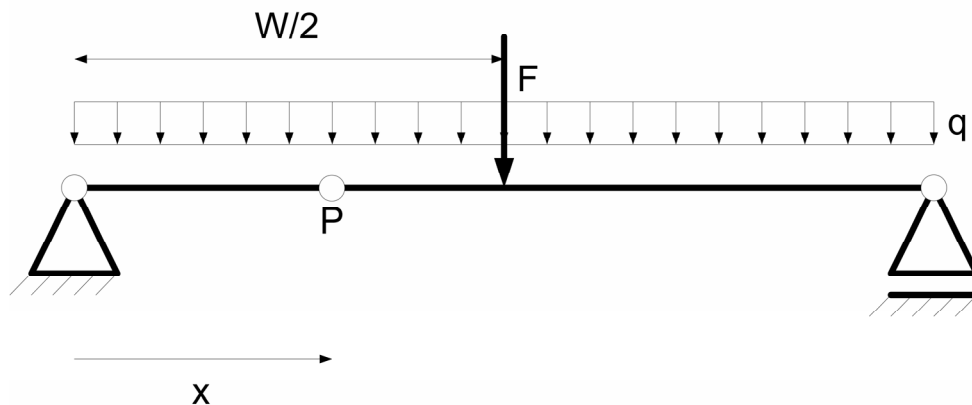


Figure 2-6: Schematic diagram of collector pipe looking into the vertical plane.

To find the maximal stresses in the pipe, a balance of forces V and moments M in the pipe cross-section at an incidental point P at a distance x from the wall bracket is set up as described by Irgens (2000 p242).

$$V(x) = \frac{1}{2}F + qL\left(1 - \frac{1}{2}x^*\right) \quad [N] \quad (3)$$

$$M(x) = \frac{1}{2}\left(F\frac{L}{2}x^* + q\left(\frac{L}{2}\right)^2\left(2x^* - x^{*2}\right)\right) \quad [Nm] \quad (4)$$

where a reduced distance x^* is introduced:

$$x^* = \frac{x}{L/2} \quad (5)$$

The normal and shear stresses are:

$$\tau_r = \frac{V}{A} \quad [MPa] \quad (6)$$

$$\sigma_r = \frac{Mr_{\max}}{I} \quad [MPa] \quad (7)$$

This is inserted into the Von Mises-criterion which yields an equivalent stress (Irgens, 1999 p102):

$$\sigma_j = \sqrt{\sigma_r^2 + 3\tau_r^2} \quad [MPa] \quad (8)$$

The equivalent stress has a maximum for $x = L/2$. This means that it is the middle joints between the collector pipes and the t-pieces that will experience the greatest strain. In this point $x=L/2$, the safety factor used for dimensioning purposes is computed from the equivalent stress and the yield stress depending on the quality of the collector pipe steel.

$$n = \frac{\sigma_j}{f_y} \quad (9)$$

2.5.3 Spring 2007: Dimensioning of turnbuckles

The same load assumptions and simplifications (see figure 2-5) are made for the spring 2007 collector probe as for the fall 2006 probe. A model of the wire rope also depends on the prestressing force. The prestressing comes from tightening the wire rope, and is done on installation of the collector probe. Estimating the prestressing is highly uncertain. Therefore, it is chosen to develop a simple model which neglects the prestressing and the elastic effects. Instead, a wall angle is assumed, and the force parallel to the wire rope is found from basic geometric considerations. The model is shown in figure 2-7. It is assumed that the force F_{res} is distributed evenly between the two wire ropes, which introduces a factor two in the denominator in equation (10).

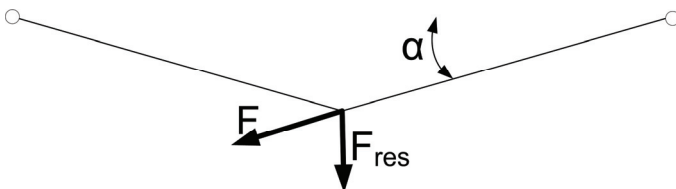


Figure 2-7: Model of wire rope based LPS collector probe.

$$F = \frac{F_{res}}{2 \sin \alpha} \quad [N] \quad (10)$$

The purpose of this model is to get some approximate values from which one can choose adequate dimensions of wire rope and turnbuckles, the latter being the weakest part of the assembly.

2.6 LPS Collector probe flow

An associated experiment was set up to find the flow through the draft tube collector. This was done by installing a pitot-static tube in a short pipe between the t-piece at the main collector and the t-piece holding the Seabird sensor. Two plastic tubes connected the pitot-static tube pressure outlets to a differential pressure transmitter placed at the draft tube gate operator's platform. The differential pressure range was set from 0-20kPa, which corresponds to a maximal velocity of 6.3m/s according to White (1999 p388). It is not likely that the pitot velocity will exceed this value, as the draft tube mean velocity stays below 3m/s.

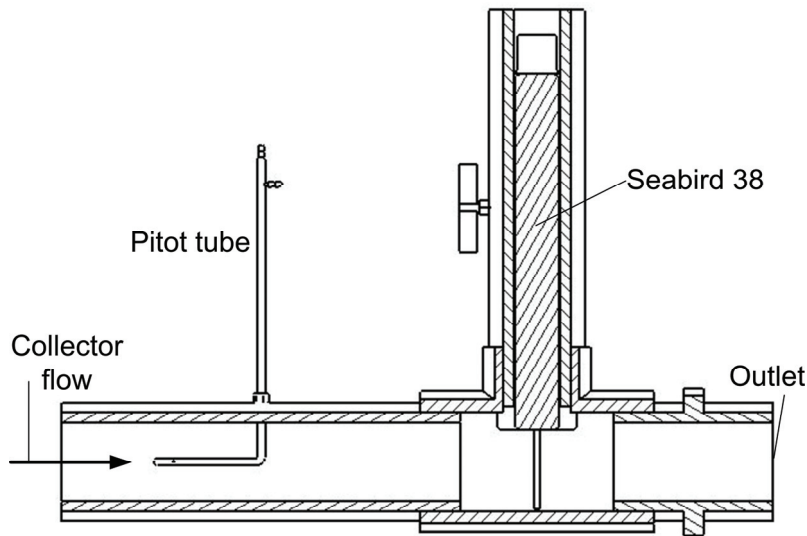


Figure 2-8: Draft tube collector flow measurement setup.

2.7 Generator efficiency

The generator efficiency at Vessingfoss has never been measured. Therefore, the generator efficiency is based on a simulation by Øivind J. Linnebo at Alstom. The simulation input was a 45 MVA rated generator with PF=0.9 at 75 degrees C and a rated voltage of 7.5kV. The simulation values are given in the table below.

Table 2-3: Simulated efficiencies for the generator at Vessingfoss.

Load	P_a	MVA	11.25	22.5	33.75	45
Generator efficiency	η_g	%	96.67	97.99	98.33	98.41

The points were used to fit a 3rd order polynomial relating the generator power with the generator efficiency:

$$\eta_g = 0.00008428P_a^3 - 0.0095605P_a^2 + 0.36533P_a + 93.65 \text{ [%]} \quad (11)$$

2.9 Leakage water flow

The flow of leakage from the upper labyrinth seal water at Vessingfoss is injected into the draft tube. During the measurements, the flow was redirected from the draft tube to the drainage basin. Redirecting the leakage water is beneficial in two ways. The water passing through the labyrinth seal is heated more than the water passing through the turbine. At Nea power station, the difference between the inlet and leakage water temperatures was 40 times higher than the difference between the inlet and outlet temperatures at BEP (Parr, 2006 app B). The leakage water has a limited time to mix with the rest of the flow, which may lead to some hot zones and as a consequence a systematic error in the temperature measurement. Redirecting the leakage water flow avoids this problem, and is also beneficial in the sense that it quantifies the leakage losses.

The drawback is that the flow and specific energy must be measured. Acoustic clamp-on meters can be used to measure flow, as the leakage water pipes are of a limited dimension. The temperature is measured in an isolated bucket where a small sample of water tapped off from the main leakage water pipe flows through at atmospheric pressure. At Vessingfoss, two different types of acoustic flow meters were tested, at two different pipe locations. All configurations failed to give results.

Both instruments showed strong variations in signal strength, which is an indicator of bubbles in the pipe flow. The presence of such bubbles was also observed at the point where the leakage water flowed out into the drainage basin.

The solution to the flow meter failure was to measure the level of the drainage basin over time, ensuring that the drainage pumps were inactive in the measuring period. The area of the drainage basin was approximated by measuring the main dimensions and the areas of the significant objects in the basin (see appendix D). A small error was also introduced as there were some other sources flowing into the basin, but this error is assumed to be negligible as the flows of these were small compared to the leakage water flow.

The flow was then computed as:

$$Q_3 = \frac{A_{Q_3} \Delta z_{Q_3}}{t} \left[\frac{m^3}{s} \right] \quad (12)$$

2.10 Index measurement setup and equations

Due to the failure of the thermodynamic test, relative efficiency values have been calculated on the basis of measured pressures and altitudes. The digiquartz pressure sensors were located on the turbine floor. The tailwater level z_2 was recorded with a pressure transducer fastened below the water level to the ladder used to access the draft tube (see figure 2-1). This point was out of the main flow, and the water level here was without major oscillations. The existing TEV remote level meter was used to measure the inlet level z_1 .

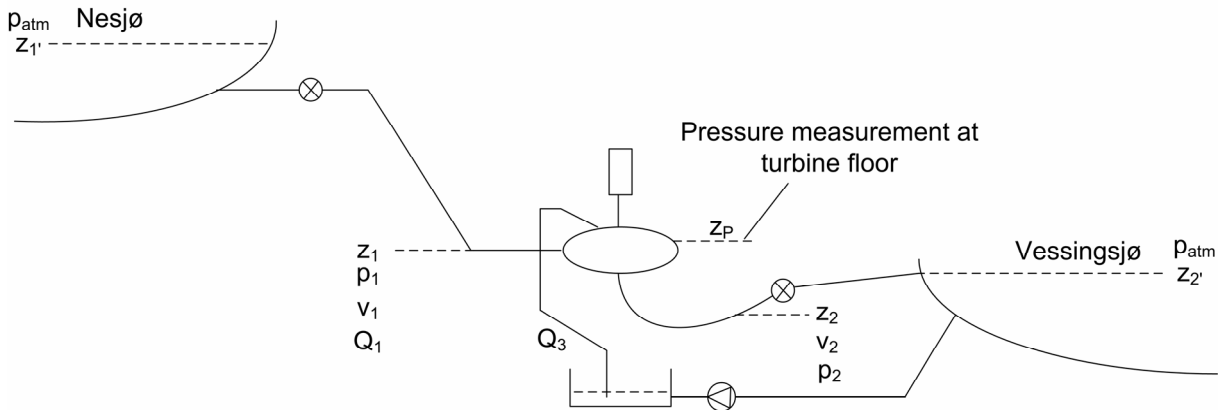


Figure 2-10: Overview of index measurement parameters at Vessingfoss.

The flow and velocities are found from Bernoulli's equation between the water at rest in the intake and the water flowing in the pipe at the point of the HPS ring pressure measurement upstream of the spiral casing (White, 1999 p.10).

$$\frac{1}{2}v_1^2 = \frac{p_{atm} + \Delta p - p_1}{\rho} + g(z_1' - z_1 - h_{head_loss}) \quad \left[\frac{m^2}{s^2}\right] \quad (13)$$

The head loss is approximated as a function of the flow squared:

$$h_{head_loss} = kQ^2 \quad [m] \quad (14)$$

Bernoulli's equation for the pipe section between the HPS ring pressure and the pressure transducer at the turbine floor is:

$$p_{1P} + \rho gz_P = p_1 + \rho gz_1 \quad [Pa] \quad (15)$$

Inserting (14) and (15) into (13) gives the HPS velocity:

$$v_1^2 = \frac{\frac{p_{atm} + \Delta p - p_{1P}}{\rho} + g(z_1' - z_P)}{\frac{1}{2} + kgA_1^2} \quad \left[\frac{m}{s}\right] \quad (16)$$

The turbine efficiency represents both the friction and impulse losses in the flow past the turbine, and the losses in the bearings due to the weight of the generator, turbine and shaft. This is slightly different from the thermodynamic method, which measures only the hydraulic efficiency.

According to the IEC (1991 p41), the turbine efficiency is:

$$\eta = \frac{P}{Q\rho E} = \frac{P_a}{\eta_g Q\rho \left(\frac{(p_1 - p_2)}{\rho} + \frac{1}{2}(v_1^2 - v_2^2) + g(z_1 - z_2) \right)} \quad (17)$$

The values of specific weight and gravity are taken to be constant and are derived from the IEC 60041:1991 appendix E.

$$\rho = 999.97 \frac{kg}{m^3}, (T = 0.5^\circ C, p = 300kPa) \quad (18)$$

$$g = 9.812 \frac{m}{s^2} \quad (19)$$

To find the initial altitude of the tailwater transducer, the height Δz between a threshold of known altitude and the tailwater level, the atmospheric pressure and transducer voltage were measured at standstill. The transducer altitude was then computed from the following equation:

$$z_{transducer} = z_{tailwater} - \frac{p_{trans}}{\rho g} = (z_{threshold} - \Delta z) - \frac{61.058V - 123.06}{\rho g} \quad [m.a.s] \quad (20)$$

2.11 Uncertainty

According to the IEC (1991 p333), the total uncertainty of the absolute method used to calibrate the index measurement becomes the systematic uncertainty of the index measurement itself. In the case where the measurement is relative, the uncertainty of the turbine efficiency is absolute, in that one does not know its magnitude. However, an analysis of uncertainty is still interesting, because it highlights the weak sides of a test, and serves to give an indication of the accuracy of the curve form.

The uncertainty analysis is based on a 95% confidence level. The total uncertainty is the RMS sum of the random and systematic uncertainty (IEC, 1991 p91). The random uncertainty of the hydraulic efficiency and turbine power can be found from a series of points made with the unit running in the same state. The random uncertainty is then evaluated by estimating the standard deviation by the sample mean, the number of points and the student's T-distribution factor (IEC, 1991 appC).

$$e_r = \frac{ts_y}{\sqrt{n}} \quad (21)$$

The equations (22) and (23) below are used for evaluation of the systematic uncertainties. They are derived from equation (17) by means of the methodology described by Storli (2006 p12-13).

$$f_{\eta} = \sqrt{f_{p_a}^2 + f_{\eta_g}^2 + f_{QE}^2} \quad (22)$$

$$e_{QE} = \sqrt{\left(\frac{\partial QE}{\partial p_1} p_1\right)^2 + \left(\frac{\partial QE}{\partial p_{atm}} p_{atm}\right)^2 + \left(\frac{\partial QE}{\partial z_1} z_1\right)^2 + \left(\frac{\partial QE}{\partial z_2} z_2\right)^2 + \left(\frac{\partial QE}{\partial z_p} z_p\right)^2 + \left(\frac{\partial QE}{\partial A_1} A_1\right)^2 + \left(\frac{\partial QE}{\partial A_2} A_2\right)^2 + \left(\frac{\partial QE}{\partial Q_3} Q_3\right)^2} \quad (23)$$

The flow multiplied by specific energy QE which is present in equation (23) is found by combining equations (16) and (17), producing equation (24). The expressions inside of the parentheses in equation (23) above are called sensitivity coefficients. For evaluation of these, the partial derivative of QE is calculated numerically in Matlab (see appendix E for Matlab code).

$$QE = A_1 \sqrt{\frac{2(p_{atm} - p_1)}{\rho} + 2g(z_1 - z_1)} \left(\begin{array}{l} \left(\frac{p_1 - (p_{atm} + \rho g(z_2 - z_2))}{\rho} \right) \\ + \left(\frac{1}{2} - \frac{A_1^2}{2A_2^2} \right) \left(\frac{p_{atm} - p_1}{\rho} + g(z_1 - z_1) \right) \\ - \frac{1}{2A_2^2} \left(Q_3^2 - A_1 Q_3 \sqrt{\frac{2(p_{atm} - p_1)}{\rho} + 2g(z_1 - z_1)} \right) \\ + g(z_1 - z_2) \end{array} \right) \left[\frac{m^5}{s^3} \right] \quad (24)$$

2.12 Head loss

The relative turbine efficiency in this report is calculated with head loss set to zero. The head loss has been calculated from station drawings to give an indication of the real efficiency value. However, calculating the head loss introduces simplifications and assumptions which make the uncertainty high, for example in estimating the roughness and the inlet and gate loss.

The geometry and calculation are shown in appendix C. Since no roughness data exist for Vessingfoss, an estimate has been made based on data from other sites. Based on values collected by Nielsen and Hulaas (1993 p10), a roughness of $\varepsilon = 0.59mm$ is found by taking the mean of three sites with steel-lined penstocks after 30-35 years of operation. Loss coefficients for losses in bends, nozzles and diffusers are derived from Idelchik (1994). The inlet loss coefficient is $K_{inlet}=0.5$ (White, 1999 p372) based on the assumption of a sharp edge. The gate loss coefficient does not in the knowledge of the author exist in literature, and is assumed to be $K_{gate}=0.1$. Both the gate and inlet loss coefficient estimates suffer because the available technical drawings do not give information on the exact geometry of the gate and inlet.

2.13 Calibration

The calibration methods of the instruments used in the index measurement are summarized in the table below. The corresponding calibration documents can be found in appendices F and G. The Digiquartz pressure transducers are calibrated externally by GE Hydro. However, the readings of the two pressure transducers deviate by a difference Δp when equal pressure is applied to the transducers. A verification of the calibration was carried out at pressures from 100kPa to 500kPa, which shows that the difference Δp is constant in the pressure operating range and equals $\Delta p=4\text{kPa}$.

The thermometers and power meter were also calibrated for the thermodynamic measurement. As this is irrelevant for the results presented in this report, it is omitted.

Table 2-4: Calibration of instruments.

Instrument	Date	Calibration place	Calibration method	Result
Digiquartz 9002K-105	17.07.2000	GE HYDRO	Dead weight tester	$\Delta p = ID01 - ID02 = 4\text{kPa}$
GE Druck PTX 1830	15.05.2007	The Waterpower Laboratory	Digiquartz 9002K	$Y = 61.058X - 123.06$ [kPa], X: [V]
Inlet level	17.04.2007	Vessingfoss	Control with measuring tape	$\Delta Z = 0.01\text{m}$

3 Results

This chapter is divided in two. First, the failure of the thermodynamic method and the inlet temperature scatter is presented. Second, the relative turbine efficiency is given as a function of turbine power, followed by a presentation of the uncertainty of this result. The relative turbine efficiency is the turbine efficiency calculated without head loss, which has been referenced to the peak efficiency value which has been set to $\eta=100\%$. The turbine power is referenced to a net head of $H=52\text{m}$ by the laws of affinity (Parr, 2006 p5). The hydraulic efficiency curve with theoretic head loss terminates the chapter.

3.1 Thermodynamic method

The first attempt at a thermodynamic measurement was carried out in October 2006. The probes had been exposed to about a month of operation between installation and measurement, and when the measurement team returned, the signal was lost from the two thermometers in the draft tube. The inspection after emptying the draft tube showed that the LPS collector probes were gone. About half of the expansion bolts fastening the brackets to the walls were gone. No measurements were made, except for pressure pulsation measurements made by Haugan (2006).

A new attempt was made in April 2007, with a modified draft tube collector design. The new design was still not good enough. The station was run from about 11am to 3pm on 19.04 without taking any measurements. This was due to errors in setting up the power meter and the acoustic flow meter. On the 20.04, the station was run from 9.30am to 14.30. During the test, signal was lost from one thermometer. After the test was over, it became clear that a collector was blocking one of the draft tube gates from reaching closed position. It was necessary for a team of divers to go down and clear out the collector debris before the draft tube gate could be set properly.

Both frames were in bad shape. The collector which still had intact thermometer and cable, was hanging only in the middle- and the floor-fastened wire ropes. The turnbuckles on the two other horizontal wire ropes were broken on the wall side. All of the turnbuckles were broken on the other collector, except for the turnbuckle bolts that were tightening the wire rope between the floor bracket and the middle of the frame.

The first run produced data from both draft tube thermometers, while the rest of the runs were made with only one draft tube thermometer. On inspection, it became clear that one frame was swept away, while the other was hanging in only one turnbuckle. This means that the results from all of the draft tube temperature measurements are unpredictable. One does not know at what time the turnbuckles have broken, or to what degree the holes in the collector pipes in the frame that was still hanging were aligned with the general flow direction, allowing water to pass by the thermometer. Nevertheless, the draft tube temperature measurements were surprisingly stable, with standard deviations in the range of:

$$s_{T_{2-1}, T_{2-2}} \in \langle 0.002, 0.009 \rangle \text{ [}^\circ\text{C]}$$

Another factor which was discovered during the test was that the inlet temperature T_{1-1} varied greatly. The range of the sample standard deviations of T_{1-1} were:

$$s_{T_{1-1}} \in \langle 0.039, 0.071 \rangle \text{ [}^\circ\text{C]}$$

The scatter was general, with no trend indicating a major temperature gradient (see figure 3-1).

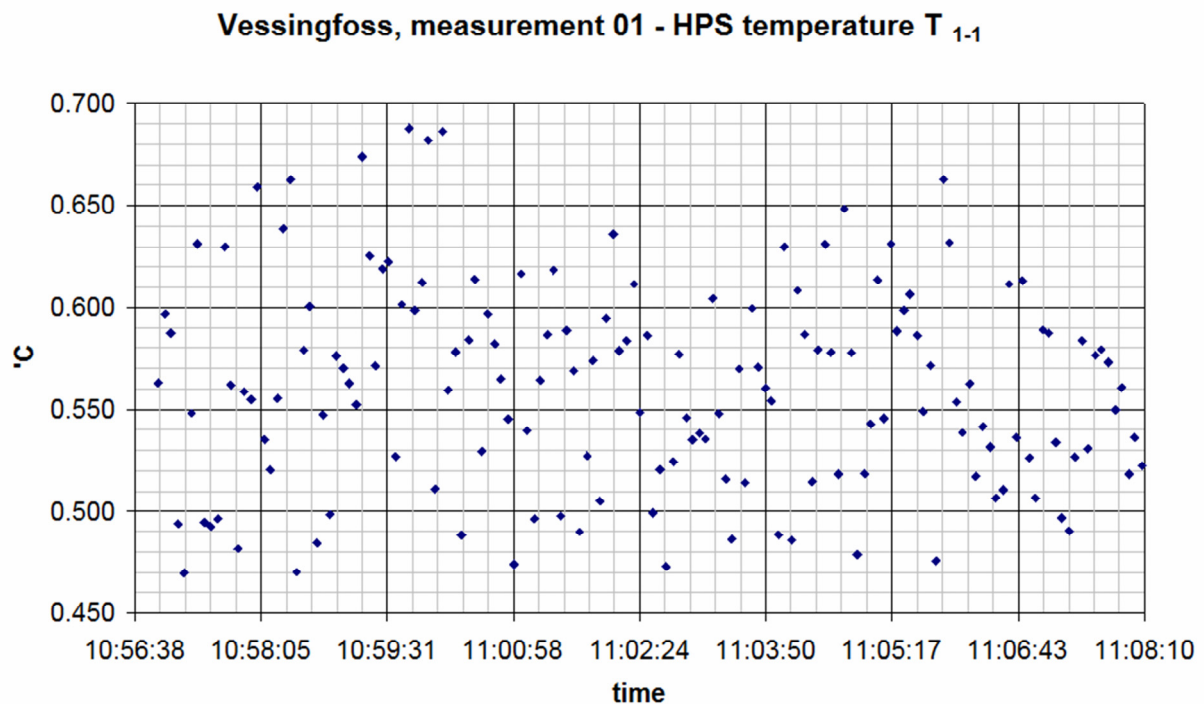


Figure 3-1: *HPS temperature scatter at Vessingfoss.*

3.1.1 The LPS collector flow experiment

The LPS collector flow experiment associated with the thermodynamic test produced no results. This was due to the fact that the pitot-static tube was broken in two when the collector took off downstream.



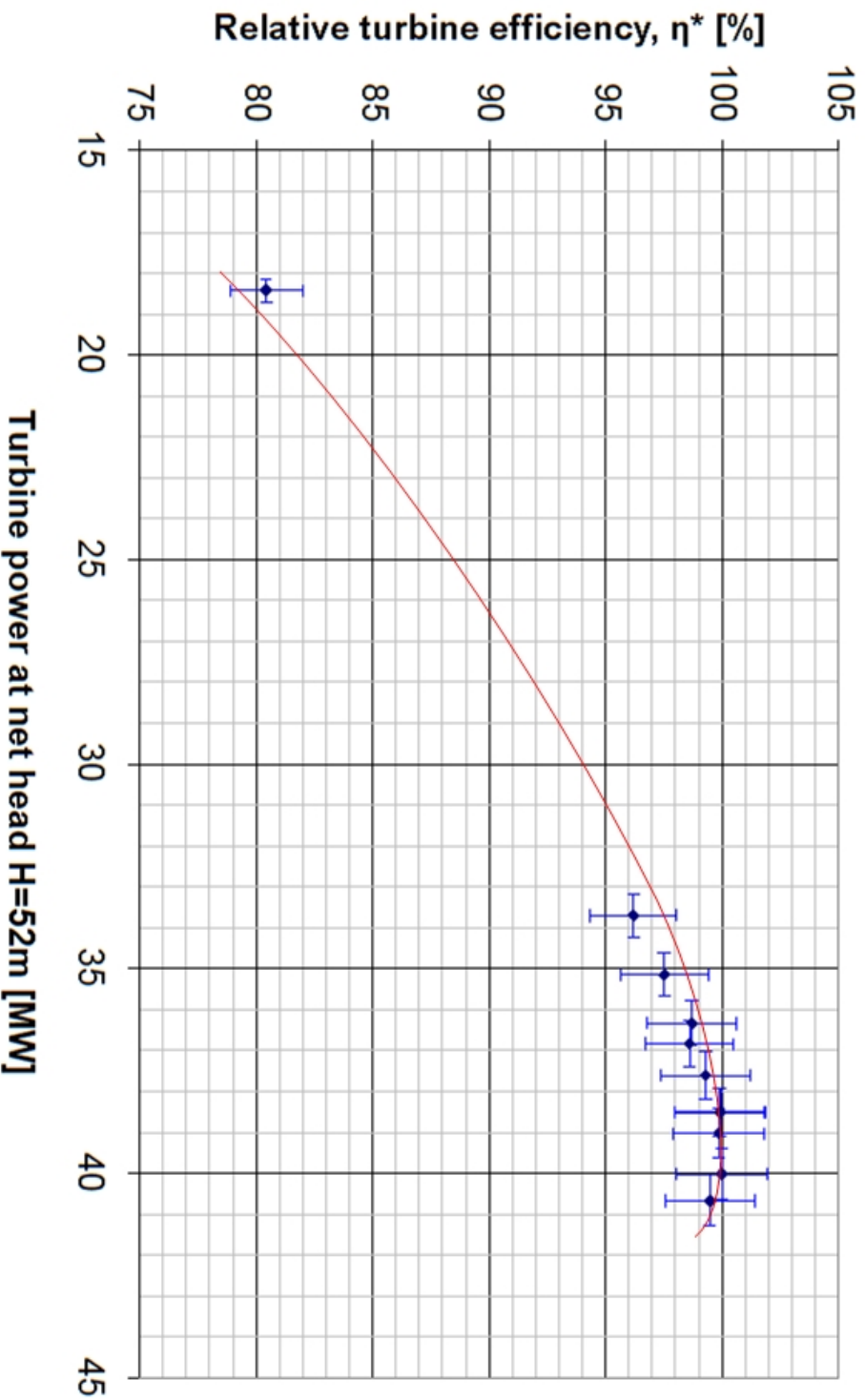
NTNU–The Waterpower laboratory

3.2 Relative turbine efficiency

Site: Vessingfoss power station

Turbine type:	Francis
Design:	Kvæerner Brug
Rated power:	40 MW
Reference head:	52 m
RPM:	214 rpm

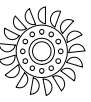
Date:	2007-20-04
Measured by:	Håkon Hjørt Francke Leif Parr
Method:	Levels and pressures(relative)
IEC-standard:	IEC 60041:1991



3.3 Uncertainty in the relative turbine efficiency

Table 3-1: Calculation and results of uncertainty analysis of the relative turbine efficiency

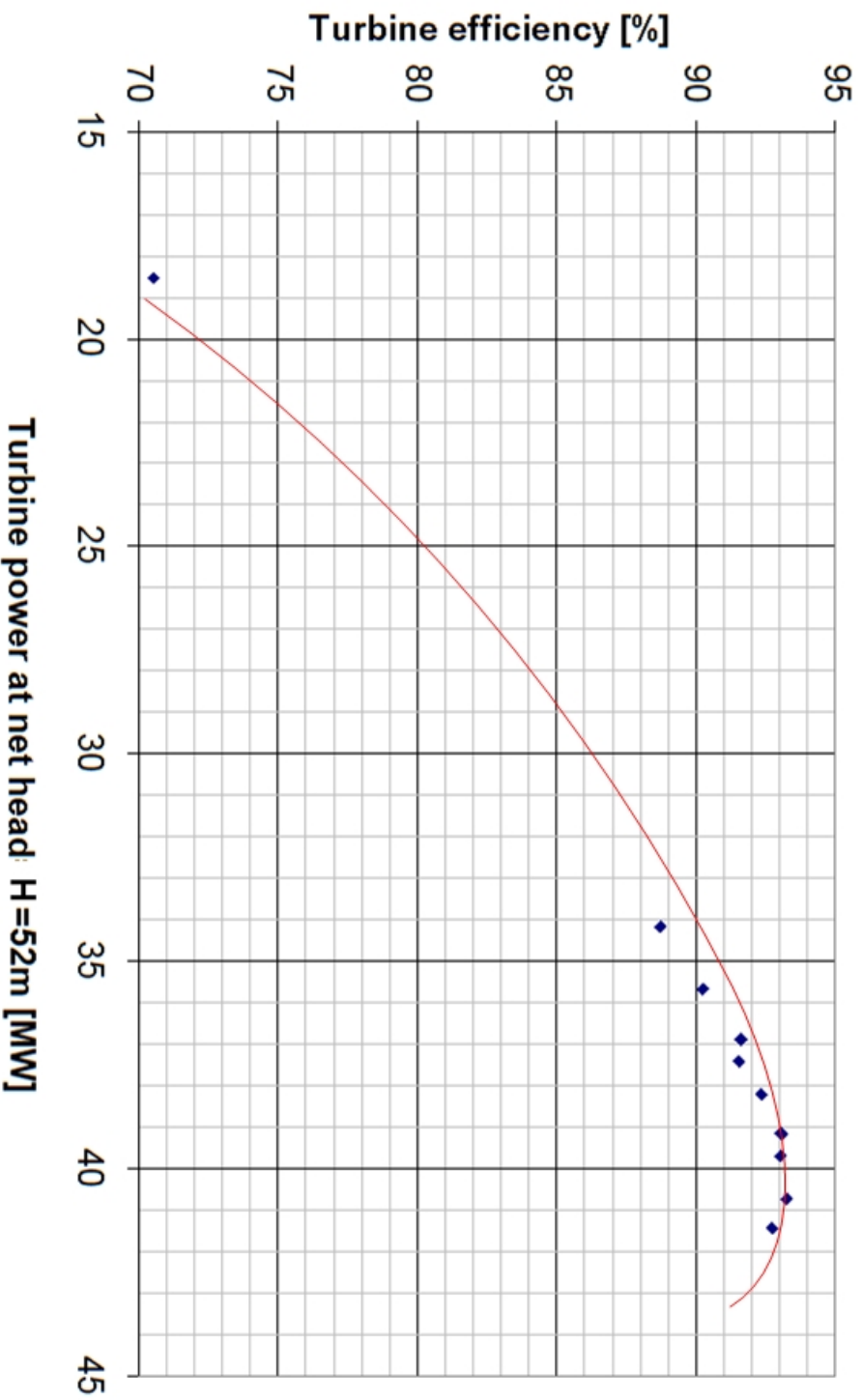
Input parameters in the systematic uncertainty			
Digiquartz 9002K-105	f_p	%	0.02
Altitudes from drawings	e_z	m	0.03
Areas from laser measurement	f_A	%	1
Nesjo level distance measurement	$e_{z1'}$	m	0.02
Water level outlet; Druck PTX and threshold level	$e_{z2'}$	m	0.1
Clearance water measurement	f_{Q3}	%	10
Generator efficiency	e_{η_g}	%	1
Generator time	f_{gt}	%	0.8
Generator rounds	f_{gr}	%	0.8
Generator constant, rounds/kWh	f_{Pg_c}	%	0.1
Systematic uncertainty in EQ			
sensitivity Patm	dEQ/dp_{atm}	m^6/kgs	1.2
error Patm	$e_{patm} * dEQ/dp_{atm}$	Wm^3/kg	21.8
sensitivity P1-measured at zp	dEQ/dp_1	m^6/kgs	0.1
error P1	$e_{p1} * dEQ/dp_1$	Wm^3/kg	15.0
sensitivity z1'	$dEQ/dz_{1'}$	Wm^2/kg	12409.0
error z1'	$e_{z1'} * dEQ/dz_{1'}$	Wm^3/kg	248.2
sensitivity z2'	$dEQ/dz_{2'}$	Wm^2/kg	-571.6
error z2'	$e_{z2'} * dEQ/dz_{2'}$	Wm^3/kg	-57.2
sensitivity zp	dEQ/dz_p	Wm^2/kg	-11837.0
error zp	$e_{zp} * dEQ/dz_p$	Wm^3/kg	-355.1
sensitivity Q3	dEQ/dQ_3	J/kg	1674.2
error Q3	$e_{Q3} * dEQ/dQ_3$	Wm^3/kg	2.3
sensitivity A1	dEQ/dA_1	Wm/kg	2613.6
error A1	$e_{A1} * dEQ/dA_1$	Wm^3/kg	303.4
sensitivity A2	dEQ/dA_2	Wm/kg	4.7
error A2	$e_{A2} * dEQ/dA_2$	Wm^3/kg	1.6
Total error EQ	e_{EQ}	Wm^3/kg	532.6
Relative uncertainty EQ	f_{EQ}	%	1.2
Relative error Pg			
Relative error Pg	f_{Pg}	%	1.1
Relative error gen.eff	f_{η_g}	%	1.0
Relative error turb.eff	f_{η}	%	1.9
Absolute Systematic error turb.eff	e_{η}	%	1.2
Systematic error turb.power	f_{Pt}	%	1.5
Random uncertainty			
Turbine efficiency	e_{η}	%	0.06
Generator power	e_{Pg}	MW	0
Generator efficiency	e_{η_g}	%	0
Turbine power	e_{Pt}	MW	0
Total uncertainty			
Turbine efficiency	f_{η}	%	1.9
Turbine power	f_{Pt}	%	1.5



3.3 Turbine efficiency with calculated head loss

Turbine type:	Francis
Design:	Kvæerner Brug
Rated power:	40 MW
Reference head:	52 m
RPM:	214 rpm

Date:	2007-20-04
Measured by:	Håkon Hjort Francke
Method:	Leif Parr
	Levels and pressures with theoretic head loss



4 Discussion

4.1 The thermodynamic method

The results of the thermodynamic test have been discarded due to two factors:

- 1) Scatter in the HPS temperature measurements.
- 2) Mechanical breakdown of the draft tube collector probes.

4.1.1 HPS temperature scatter

The standard deviation of T_{1-1} was greater than the expected temperature difference over the turbine. In addition, the mean did not converge towards a value when logged over a long period $t > 10\text{min}$, which indicates a transient instability in the temperature.

The measured temperature difference over the turbine was approximately a factor ten higher than expected. In point number one, the difference was:

$\Delta T = \text{mean}\left(T_{2-1}^-, T_{2-2}^-\right) - T_{1-1}^- = 0.118^\circ\text{C}$, which would give a hydraulic efficiency of $\eta_h = 1.6\%$ according to the equations used by Parr (2006 p3-5). This is obviously erroneous.

The reasons for the scatter are yet to be established. Two hypotheses to the cause of this problem have been suggested. The first is a known problem with the thermodynamic method and concerns temperature layers in the reservoir. The second hypothesis is that the HPS probe is subject to backflow. The cause of this eddy could possibly be the 50 degree bend located upstream of the HPS probe. Idelchik (1994 p339) gives the length of the flow separation zone at the inner wall for a 90 degree bend at Reynolds numbers greater than $Re_d \geq 0.3 \times 10^6$ (see figure 4-1 below). Inserting the Vessingfoss pipe diameter gives a flow separation zone length of 4.4m. The Vessingfoss bend only is 50 degrees, and the curvature is less than the Idelchik geometry curvature, thus the real zone will be considerably shorter than 4.4m. The HPS probe is located about 10m downstream of the bend, and it is therefore unlikely that it is subject to backflow due to the bend.

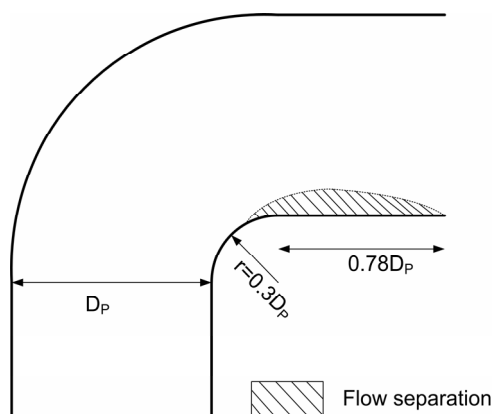


Figure 4-1: Flow separation at the inner wall of a 90 degree bend with $Re_d \geq 0.3 \times 10^6$. (Idelchik, 1994)

There is a possibility that temperature layers in lake Nesjø cause variations in the inlet temperature. In most lakes there is a thermocline, which is an abrupt change of water temperature in depth (Wikipedia, 2007). In a situation where the thermocline is located in the middle of the intake, water from both temperature layers will enter the penstock. The Vessingfoss penstock is short, and temperature mixing before the water reaches the HPS probe is limited.

Since the thermocline will move when water is drained from the lake, one can expect the scatter situation to improve over time. To explore this possibility, the thermometer in the HPS probe was left to record after the test was finished. Unfortunately, due to planned dam maintenance in lake Vessing, Vessingfoss was to be operated minimally in the period between the test and fall 2007. Two weeks after the test was completed, the station was run for a period of eleven hours, after which TEV no longer would operate. There was little improvement of the inlet temperature scatter during this measurement. The standard deviation of the inlet temperature dropped from about 0.055°C to 0.038°C in eleven hours. This remains out of useful range, compared to results from measurements at Nea power station fall 2006, which had standard deviation levels of temperature of about 0.004°C, most of which was due to an overall temperature gradient during the measurement period. Considering that lake Nesjø is quite big, and it may take a considerable amount of time to draw off enough water for the thermocline to move, the recording period was too short for the results of this investigation to be conclusive.

A way to establish the location of the thermocline is to measure the temperature depth distribution in lake Nesjø. This idea was not considered in due time, and no measurements were made. In connection with water quality tests in lake Nesjø, TEV has measured the water temperature at different depths. These tests have been carried out spring and fall every other year from 1992-2006. The results from those of the tests taken in April have been investigated. Unfortunately, the temperature measurements have not been taken with adequate resolution and depth to be useful to this discussion.

Further investigation into the temperature layer hypothesis is necessary before conclusions can be drawn. This should be done by measuring the temperature depth distribution of lake Nesjø at depths well below the intake and with a resolution smaller than 1m, and by recording the HPS temperature over several weeks.

4.1.2 Draft tube collector probes-fall 2006.

The collector probes and thermometers were found by divers on the downstream side of the draft tube gates in April 2007. Inspection of the frame showed that some pipes were cut off in the threaded section in the joint with the t-pieces and central manifold. The most probable chain of events is that first the pipes have broken in the central joints. Afterwards, the expansion bolts in the wall have been loosened and pulled out by the movement of the cut-off pipes in the free stream.

The method for dimensioning the 2006 collector probe fails to predict the breakdown. The results of the calculations are given in table 4-1 below. All assumptions in the calculations are conservative, and the factor of safety of 8.8% is by good margin on the safe side of the hydropower industry standard, which is 40%. One weakness of the model is that it does not take into account the threaded parts of the pipes in the position of greatest strain. This could be improved by including a stress concentration factor. On the other hand, as the assumptions underlying the load are of high uncertainty, going into such detail might be a waste of time. This also holds true as the pipes used for this purpose often are bought uncertified, which means that exact values of yield stress and stress concentration factors do not exist.

Table 4-1: Input and results from design of Vessingfoss LPS collector probes.

Dimensioning velocity	v	m/s	6
Pipe, inner diameter	D _i	mm	52
Pipe, outer diameter	D _o	mm	60
Fall 2006			
Length	W	mm	3435
Height	H/3	mm	923
Von mises-max	σ_j	MPa	17.5
Yield stress	f _y	MPa	200
factor of safety	n	%	8.8
Spring 2007			
Length	W	mm	3000
Height	H/3	mm	923
Angle between wall and wire rope	α	Deg	4
Resultant orthogonal force	F _{res}	kN	4.2
Force component along wire rope	F	kN	30.4
Turnbuckle work load limit SO WLL	F _{limit}	kN	4.9

4.1.3 Draft tube collector probes-spring 2007

It is quite clear that the turnbuckles were the weak component in the wire rope collector solution. TEV and the Waterpower Laboratory both agree that the turnbuckles were under-dimensioned.

However, the wire rope solution still is interesting, in that it is easy to install, and that the collector pipes may be scaled down. All of this needs further investigation, and the solution needs to prove itself.

The model used for validating the turnbuckles is quite simple, and has limitations. The most obvious limitation is the sensitivity of the force along the wire rope to the choice of the wall angle. Nevertheless, this simple calculation could have foreseen the breakdown of the turnbuckles. The turnbuckles at Vessingfoss were uncertified, and even though the work load limit was printed on them, it is hard to say if this value is trustworthy. For future wire rope collectors, one must aim at buying certified components, so that yield stress and load can be compared with a certain degree of predictability.

4.2 Index measurement

According to Muciaccia and Walter (2000), the main goal of index tests is to obtain reliable relative efficiency curves and to optimise blade and gate cam curve. The latter applies only to Kaplan turbines. A reliable relative efficiency curve was not the goal of TEV when they initiated the thermodynamic test. The only immediate use of the relative efficiency is to confirm the location of the BEP (see table 4-2). This coincides with the analytical results of Hulaas (2001), and also with the instructions of the TEV control centre.

Table 4-2: Comparison of index test BEP with analytic BEP from Statkraft Grøner.

BEP index test 2007	H=52m	P=39MW
BEP analytic Hulaas 2001	H=50m	P=37MW
BEP analytic Hulaas 2001	H=55m	P=41.5MW

4.2.1 Efficiency with head loss

The turbine efficiency with theoretic head loss is $\eta=93.2\%$ at BEP. For comparison one can look to Gordon (2001), who has developed a method to estimate the peak hydraulic turbine efficiency based on statistical analysis of data from existing turbines. Inserting the Vessingfoss design values into Gordon's formula gives a peak hydraulic efficiency of $\eta_h=93.3\%$. Multiplying the hydraulic efficiency by the mechanical efficiency will produce a somewhat lower turbine efficiency. The mechanical efficiency ranges according to Raabe (1985 p345) from $\eta_m=98\%$ to $\eta_m=99.5\%$. Using a mean value of these, the Gordon turbine efficiency becomes $\eta=92.1\%$. Given the uncertainties of both methods, the Gordon efficiency and the measured efficiency with calculated head loss are in accordance.

This comparison strengthens the head loss calculation and the assumptions made. The gate loss coefficient, which is the weakest assumption, is not completely on the wrong track.

4.2.2 Rejection of outliers

Point number 4 ($P_t=38.4\text{MW}$; $\eta^*=98.0\%$) has been rejected. The background for rejecting the point is that it deviates from the curve form suggested by the rest of the points. Looking at the servo stroke curve, which has been measured as a control value (see appendix B), it is clear that something is incorrect in point 4. An increase of 1MW in the point 4 generator power agrees with the servo stroke curve, and when efficiency is calculated, it fits well into the general curve form. It is therefore probable that the generator power measurement is faulty in this point.

4.3 Uncertainty

The total uncertainty of the turbine efficiency at BEP is $e_\eta=\pm 1.6\%$. This is higher than the uncertainty $e_{\eta_h}=\pm 1.15\%$ of the thermodynamic measurements at Svean power station (Francke and Wiborg, 2005). In general, before an experiment is made, emphasis is put on locating the main sources of uncertainty and minimizing these by using equipment of adequate precision (Holman, 1971 p25). This was done at Vessingfoss with regard to the thermodynamic test. The index test was only a backup solution, and has seen no such analysis.

4.3.1 Random uncertainty

The random uncertainty of the hydraulic efficiency and turbine power was found from three points made while the unit was running in the same state, points 11 through 13.

The observant reader might object to the fact that the random uncertainty has been evaluated in three runs close to BEP. This is where the turbine runs in its most stable state, with few transients in the properties measured. This said, the points in the Vessingfoss test were all except one recorded around BEP, which implies that the values of random uncertainty are valid for most points. The evaluation is done mostly to establish that the random uncertainty is negligible, as is shown in previous measurements. At Nea, for example, the random uncertainty was small compared to the systematic uncertainty (Parr, 2006 App-p11).

In this measurement, the random error associated with the turbine efficiency and turbine power is negligible compared to the systematic error.

4.3.2 Systematic uncertainty

The generator power, generator efficiency, specific energy and flow contribute nearly equally to the systematic uncertainty. The uncertainty in the generator power could have been reduced if the external power meter connection would have been successful.

The specific energy E and the flow Q together contribute the most to the systematic uncertainty. In the calculation, they are grouped together because they depend on the same measured quantities. Looking at the sensitivities and uncertainties in the energy and flow, it is clear that the uncertainty in the inlet level z_1 , the pressure measurement level z_p and the area A_1 are the most important.

The altitude of the pressure measurement is found from technical drawings. Trusting technical drawings, which in this case date back to the 1970's, can have surprising results. This was the case when TEV manufactured stop logs for work on the Sylsjøen mini hydro project in the spring of 2007. The diving team quickly discovered that the stop logs dimensioned from drawings did not fit into place and had to be modified, slowing down the project. This illustrates that it is undesirable to have to rely on drawings, especially when it is difficult to double-check the numbers. It is also difficult to estimate the systematic uncertainty of such altitudes, which in this report is set to $e_z = \pm 3\text{cm}$.

The inlet level is measured using the existing TEV Nesjø level measurement. A control measurement (appendix G) showing good accordance ($\pm 1\text{cm}$) had been carried out on the day before the measurements, giving an indication of the uncertainty. This was only a stroke of luck, as z_1 was thought to be a control parameter for the thermodynamic test, in the calculation of which the parameter is not needed. Therefore, no effort was made beforehand to ensure that z_1 be accurate. In general, relying on on-site equipment can present a problem of finding and validating calibration data.

The accuracy of the HPS area is hard to improve. The measurements of the diameters show that the cross-section at the entrance to the spiral casing is not 100% circular. This introduces an error which is hard to evaluate. Other methods might be more accurate, as described by Vassdragsregulantenenes Forening (1986), such as the photographic- or rotating laser methods. However, these methods use expensive equipment, and are time consuming.

4.4 Observations at Vessingfoss

A number of observations were made at Vessingfoss during the test. The most significant are discussed below.

4.4.1 kWh-counter and measurement transformers

The accuracy of the kWh-counter is taken as a precaution against the index measurement. According to TEV, the counter is checked against an external energy meter on a regular basis. Still, an informal check of the kWh-counter power to the power registered externally as by the TEV operations centre, showed a deviation of 1MW. As this comparison itself was rather makeshift, it is not taken into account in evaluating the uncertainty of the power measurement.

Another indication that questions the reliability of the kWh-counter, and also the other station instruments, is the inexplicable behaviour of the measurement transformer electric circuit when attempting to connect the external power meter. The voltage transformer values were as expected. The current circuits of both the kWh-counter and the control room instruments were unbalanced, meaning that the neutral wire current was significant. The power measured by the external power meter by the three wattmeter method was obviously incorrect. However, the source of the above may also be either a faulty connection of the power meter, or an error in the power meter itself. TEV electrical personnel and the measurement team worked together and double-checked each other in all connections, and one can safely assume that there was no error on this part. The connection was based on technical drawings. There is a possibility that the electric system has been modified without updating the drawings, which may explain the error. The possibility of an error in the power meter itself is small. It was calibrated in December 2006, and used flawlessly in a three-wattmeter power measurement in Korea. There, it measured the exact same values as the station kWh-counter.

Considering the above, TEV should look into the two current transformers used for station measurements at Vessingfoss. It is important to establish the reliability of the kWh-counter and measurement transformers for an eventual later measurement. There was also trouble with the measurement transformers at Nea (Parr, 2006 p11), which means that Vessingfoss may not be an isolated case.

4.4.2 Gas bubbles in the leakage water

The gas bubbles in the leakage water perturbed the acoustic measurement of the leakage water flow. The source of the bubbles may be an air inlet pipe, which according to the overview drawing of the turbine (see figure 4-2) passes by the low pressure side of the upper labyrinth seal. A leakage from this pipe to the water could explain the amount of gas in the leakage water.

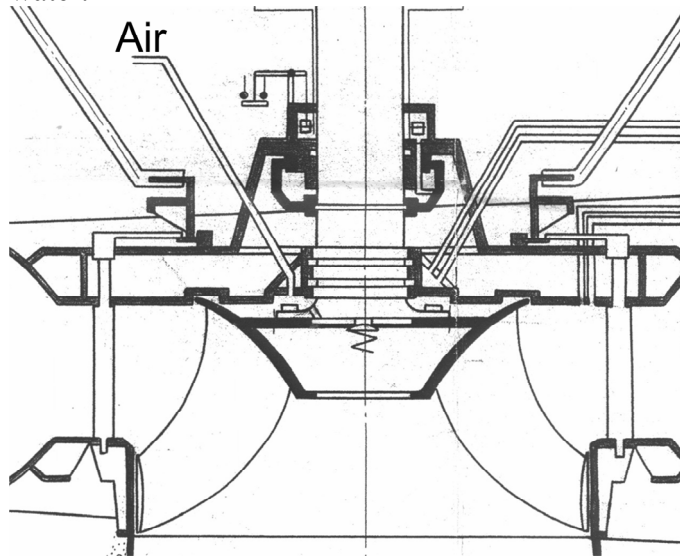


Figure 4-2: Section view of Vessingfoss turbine from general technical drawing.

4.4.3 Draft tube surge tank and cavitation

During installation in the draft tube, it was observed that water was coming down continuously from an aeration chamber above the draft tube. The outlet of this chamber comes down into the roof of the draft tube about half way between the draft tube's lowest point and the island before the gates. The original function of this chamber might have been to accommodate a bypass safety valve that was never installed. In addition, a drainage pipe from the transformer room came down here. The original design was modified due to leakage problems in this pipe, so that the transformer drainage pipes are now directed to the drainage basin. This means that this chamber now serves only as a surge tank. The chamber can be purged through a valve located on the turbine floor, but this isn't always done before start-up. Running the unit with air in the surge tank will modify the dynamic performance of the system. In a worst case scenario, the frequency response of the surge tank is equal to the frequency of the pressure pulsations, thus contributing instead of dampening them. Since the amount of air in the surge tank is unknown, there is no way of controlling its dynamic properties. It is therefore recommended that the tank should be purged as a part of the start-up procedure.

In addition, a hole in the concrete was observed in the bottom of the draft tube under the turbine, probably due to cavitation. The hole is about 10cm deep. Since the problem of pressure pulsations comes from both the turbine and draft tube, and the draft tube losses make up a significant part of the total hydraulic turbine losses (Dahlhaug, 1997 p2), the gains of simple draft tube maintenance to get rid of such irregularities are not to be underestimated.

5 Further work

5.1 Further measurements at Vessingfoss: Gibson’s method

The thermodynamic test has failed to fulfil the TEV aspirations of obtaining reliable turbine efficiency data of the Vessingfoss turbine. It is reasonable to look for other possible measurement methods, of which the most relevant alternative is Gibson’s method, also referred to as the pressure-time method. A thorough description of the method is given by Francke and Wiborg (2005) and Adamkowski et. al (2006). It requires transient pressure measurements at two different cross-sections in the penstock. Francke and Wiborg’s experience from Svean shows that the installation in the penstock takes several days, and that a specially tailored trolley must be procured to enable work in the penstock. It might be possible to reuse the equipment employed at Svean for this purpose.

5.2 Installation of Winter-Kennedy pressure tapplings

If another measurement is to be made, it is recommended to install Winter-Kennedy pressure tapplings in the spiral casing. The Gibson measurement can be used for calibration of the Winter-Kennedy constants. Measuring the Winter-Kennedy pressure, levels and the power output saves a great deal of time in subsequent measurements, as there is no need for

installation of equipment in the waterways. According to the IEC recommendations (see figure 5-1), installing the outer tap should be straightforward, as there is access to this part of the spiral case from the turbine floor. The inner tap, however, might require a bigger effort. This should be considered by TEV.

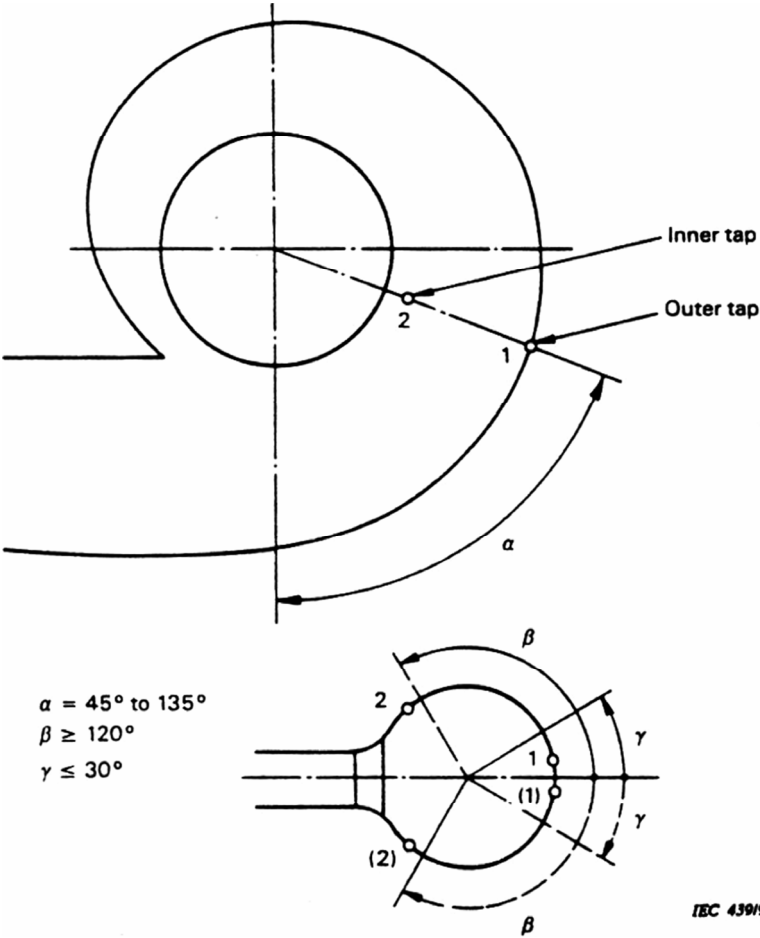


Figure 5-1: Location of taps for the Winter-Kennedy method of discharge measurement through a turbine equipped with a steel spiral case (IEC, 1991 figure 66).

6 Conclusion

Two measurement attempts by the thermodynamic method at Vessingfoss have failed, due to HPS temperature scatter and mechanical breakdown of the LPS collector probes. The result of the test is the relative turbine efficiency calculated by pressures and levels. This only serves to support the location of the BEP simulated by Hulaas (2001).

The uncertainty of the relative turbine efficiency is high. The errors in the generator efficiency, the specific energy and the flow are due to parameters which are hard to improve. This method of measurement should only be used as a backup.

The reasons for the inlet temperature scatter are yet to be found. The investigation of this thesis does not go deep enough into the problem to draw conclusions. It is unlikely that it is due to the thermocline in lake Nesjø or the fifty degree bend in the bottom of the penstock.

TEV should switch to Gibson's method for further measurements. In conjunction with this, Winter-Kennedy pressure tapings should be installed.

Retrospectively, had inlet temperature measurements been carried out in October 2006, the scatter problem could have been detected at an earlier stage, and by switching methods, a successful spring 2007 test would have been possible. The measurement team can hardly be blamed for not being adequately vigilant, as this kind of temperature scatter is quite unusual in Norwegian power stations.

Other recommendations for the Vessingfoss power station are that the hole in the draft tube floor should be filled, the draft tube surge tank should be aerated as part of the start-up procedure, and control of both of the current transformers for the station instruments should be carried out. The latter is an important point before another test is to be made.

Bibliography

- Dahlhaug, O. G. 1997. *A study of swirl flow in draft tubes*. Ph. D. thesis 1997:130, Norwegian University of Science and Technology.
- Dahlhaug, O. G and Brekke, H. 1996. Energy distribution at the draft tube outlet. In: *The International Group for Hydraulic Efficiency Measurements meeting*, 1996, Montreal. Place of publication: www.ighem.org
- Francke, H. H and Wiborg, E. J. 2005. *Falltaps- og virkningsgradsmålinger ved Svean Kraftverk*. Master thesis, Norwegian University of Science and Technology.
- Gordon, J. L. 2001. Hydraulic turbine efficiency. *Canadian Journal of Civil Engineering*, **28**, p238-253.
- Haugan, K. 2006. *Francisturbiner – slitmekanismer og kostnader ved kjøring utenfor bestpunkt*. Master project, Norwegian University of Science and Technology.
- Holman, J. P. 1971. *Experimental methods for engineers*. USA: McGraw-Hill.
- Hulaas, H. 2001. *Vessingfoss Kraftverk: Vurdering av virkningsgrad, vannforbruk og kavitasjon*. Report from Statkraft Grøner to TEV Kraft AS avd Nea-verkene.
- Idelchik, I. E. 1994. *Handbook of Hydraulic resistance*. The USA: CRC Press, inc.
- Iliescu, M. S, Ciocan, G. D. and Avellan, F. 2002. 3D PIV and LDV measurements at the outlet of a Francis turbine draft tube. In: *The joint US ASME – European fluids engineering summer conference proceedings, July 14-18 2002, Montreal*. FEDSM2002-31332.
- Irgens, F. 1999, 6th ed. *Fasthetslære*. Trondheim: Tapir Forlag.
- Irgens, F. 2000, 6th ed. *Statikk*. Trondheim: Tapir Forlag.
- Kjølle, A. 2003. *Hydraulisk måleteknikk*. Trondheim: The Waterpower Laboratory, NTNU.
- Muciaccia, F. F. and Walter, R. B. 2000. Evaluation of the benefits of turbine refurbishment by means of index test method. Reliability of results and problems in application. In: *3rd IGHEM international conference proceedings, July 2000, Kempten*.
- Nielsen, T and Hulaas, H. 1993. Optimum refurbishment time for power plant penstocks. In: *Conference papers. Waterpower and dam construction conference, 1993, Florence*.
- Parr, L. 2006. *Turbinvirkningsgrad og falltap ved Nea kraftverk*. Master project, Norwegian University of Science and Technology.
- Prasad, A. K. 2000. Stereoscopic particle image velocimetry. *Experiments in Fluids*, **29**, p103-116.

Raabe, J. 1985. *Hydro Power. The Design, Use, and Function of Hydromechanical, Hydraulic and Electrical Equipment*. Düsseldorf: VDI-Verlag GmbH.

Storli, P. T. 2006. *Modelltest av Francis turbin i Vannkraftlaboratoriet*. Master thesis, Norwegian University of Science and Technology.

The International Electrotechnical Commission. 1991. IEC 60041, 3rd ed. *Field acceptance tests to determine the hydraulic performance of hydraulic turbines, storage pumps and pump-turbines*. Geneva : IEC.

Vassdragsregulantenenes forening, teknisk sektor. Unpublished, 1986. *Falltap i kraftverkstunneler*. Report dated February 1986.

Vekve, T. 2004. *An experimental investigation of draft tube flow*. Ph. D. thesis 2004:36, Norwegian University of Science and Technology.

White, F. M. 1999. *Fluid Mechanics, 4th ed*. Singapore: McGraw Hill.

WIKIPEDIA. 2007. Thermocline [online]. [Accessed 13.06.2007]. Available from World Wide Web: <<http://en.wikipedia.org/wiki/Thermocline>>

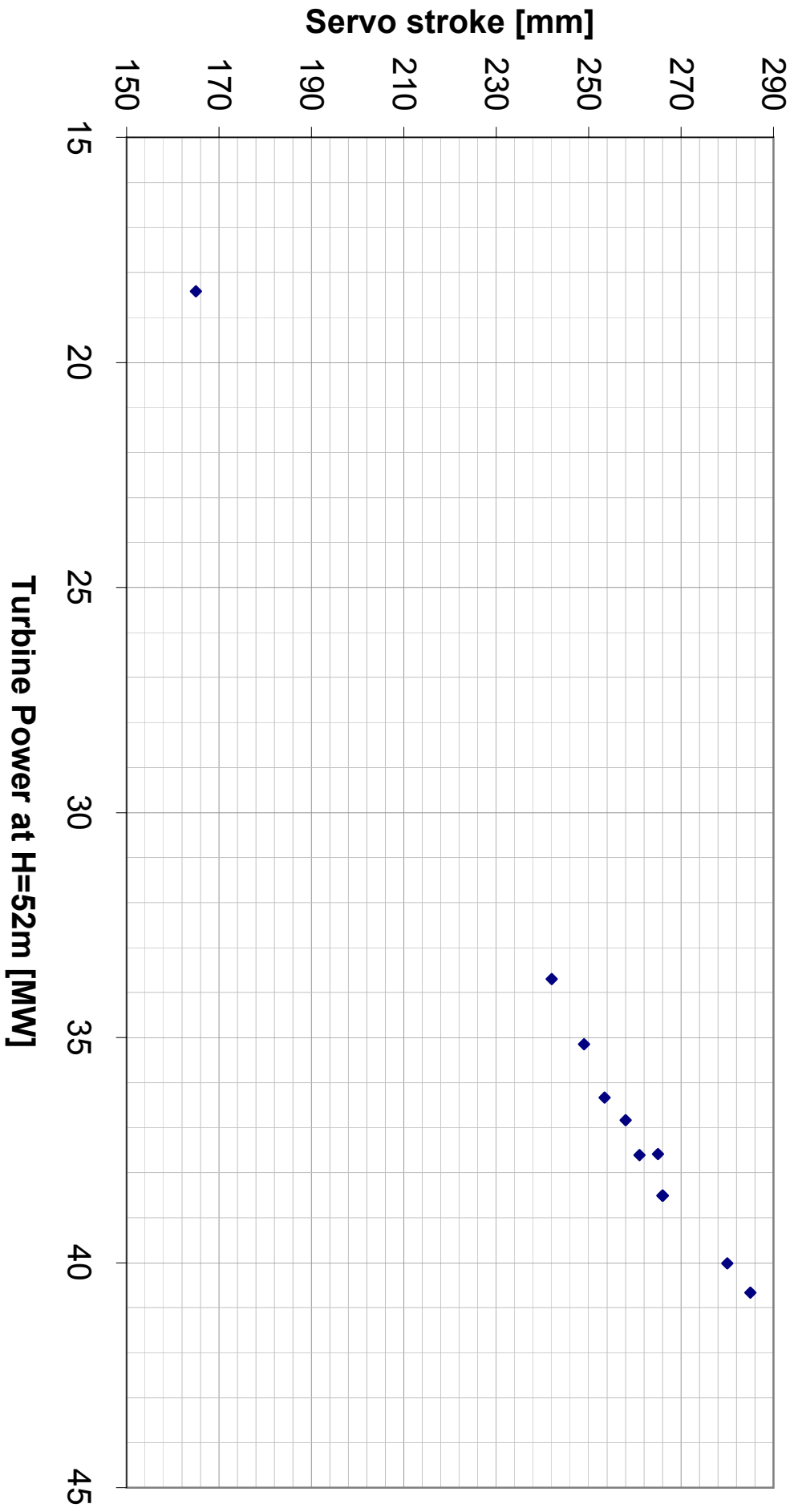
Appendix

A	Vessingfoss April 2007: Data	1
B	Vessingfoss April 2007: Servo stroke	2
C	Calculation of head loss at Vessingfoss	3
D	The clearance water basin at Vessingfoss	5
E	mydiff.m – a numerical derivation function for Matlab 7.0.....	6
F	Calibration of tailwater pressure transducer.....	8
G	Inlet altitude calibration	9

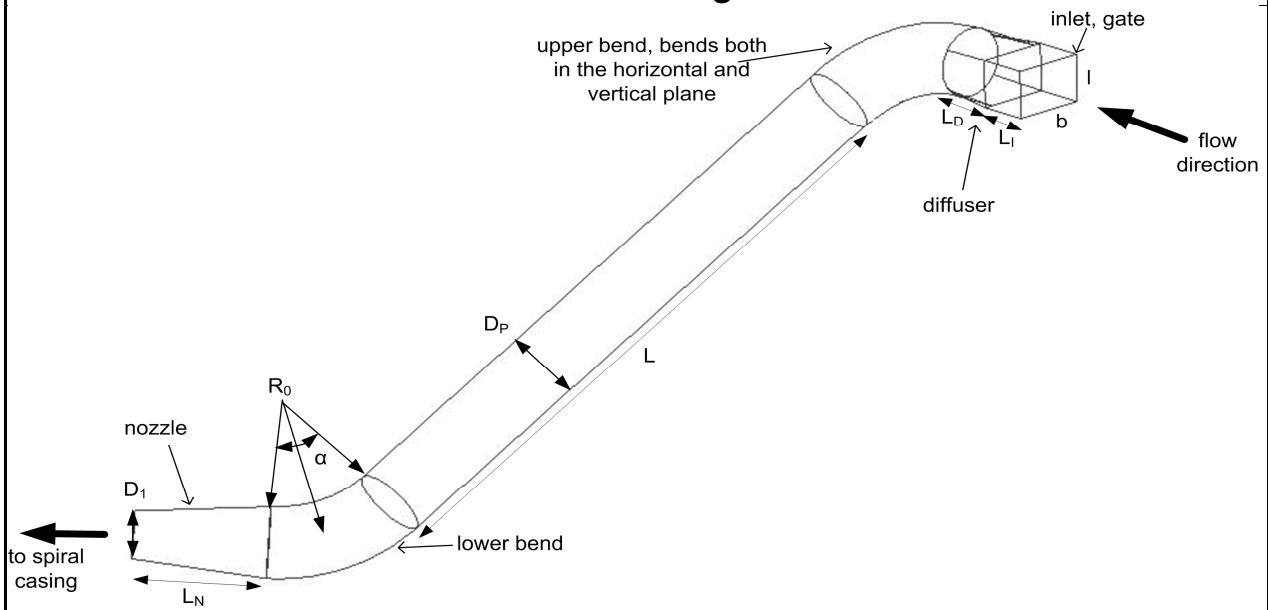
Vessingfoss April 2007: Data

Altitudes	Measurement	1	2	3	4	5	6	7	8	9	10	11	12	13
		Head water level	z ₁	m.a.s	723.77	723.77	723.77	723.76	723.76	723.76	723.75	723.75	723.75	723.75
Tailrace level	z ₂	m.a.s	671.18	670.99	670.27	671.29	671.39	671.44	671.34	671.26	671.23	671.14	671.31	671.31
Pressures														
Atmospheric	P _{atm}	kPa	90.2	90.3	90.3	90.3	90.4	90.4	90.4	90.4	90.4	90.4	90.5	90.5
HPS centre line	P _{lp}	kPa	595.8	598.2	612.1	593.4	591.0	589.5	592.5	594.3	595.0	596.9	593.3	593.4
Power														
Generator output	P _a	MW	36.0	33.6	18.7	37.1	39.3	39.9	38.4	37.1	36.4	34.9	38.0	38.0
Reactive power		MVAR	-1	-2	-2	-1	-1	-1.5	-1	-2	-2	-2	-2	-1
Clearance water flow	Q ₃	m ³ /s	0.016	0.016	0.013	0.016	0.015	0.015	0.015	0.016	0.016	0.016	0.015	0.015
Results														
HPS flow	Q ₁	m ³ /s	88.1	84.5	58.3	91.8	95.3	97.3	93.1	90.4	89.4	86.5	91.9	91.8
Turbine head	H	m	52.3	52.5	53.4	52.1	52.0	51.9	52.1	52.1	52.2	52.3	52.1	52.1
Relative turbine efficiency	η*	%	98.7	96.2	80.4	98.0	100.0	99.5	99.9	99.3	98.6	97.5	99.9	99.9
Turbine power, H=52m	P ₀	MW	36.3	33.7	18.4	37.6	40.0	40.7	39.0	37.6	36.8	35.1	38.5	38.5
Uncertainty														
Turbine efficiency	ε _η	%	1.6	1.5	1.2	1.6	1.6	1.6	1.6	1.6	1.6	1.5	1.6	1.6
Turbine power	ε _p	MW	0.6	0.5	0.3	0.6	0.6	0.6	0.6	0.6	0.6	0.5	0.6	0.6

Vessingfoss April 2007: Servo stroke



Calculation of head loss at Vessingfoss

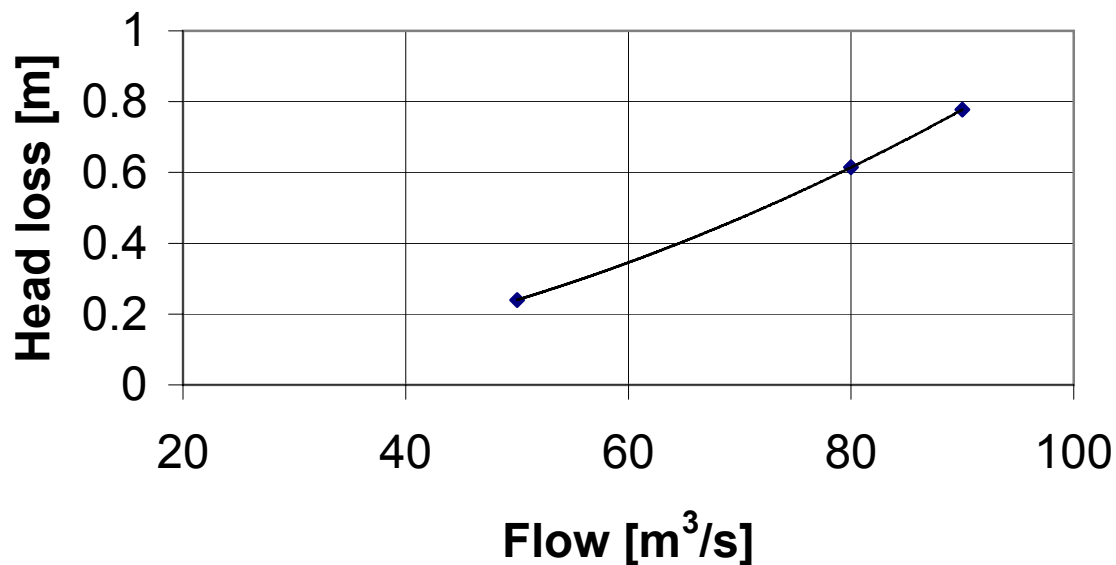


Geometry and properties			
Roughness	ϵ	mm	0.59
Specific weight water at 0.5°C p=300kPa	ρ	kg/m ³	999.97
Viscosity of water at 1atm, 0°C	μ	kg/ms	1.79E-3
Gravity at Vessingfoss	g	m/s ²	9.82
Inlet			
Inlet height	l	m	5.8
Inlet width	b	m	4.0
Inlet hydraulic diameter	D_{H-i}	m	4.7
Inlet length	L_i	m	3.8
Diffuser length	L_D	m	4.5
Upper bend			
Bend radius	R_0	m	12.7
Bend angle	α	deg	58
Penstock			
Diameter penstock	D_p	m	5.70
Length penstock	L_p	m	37.2
Lower bend			
Bend radius	R_0	m	11.4
Bend angle	α	deg	50
Nozzle			
Nozzle length	L_N	m	10.0
Nozzle outlet/spiral casing inlet diameter	D_1	m	3.8

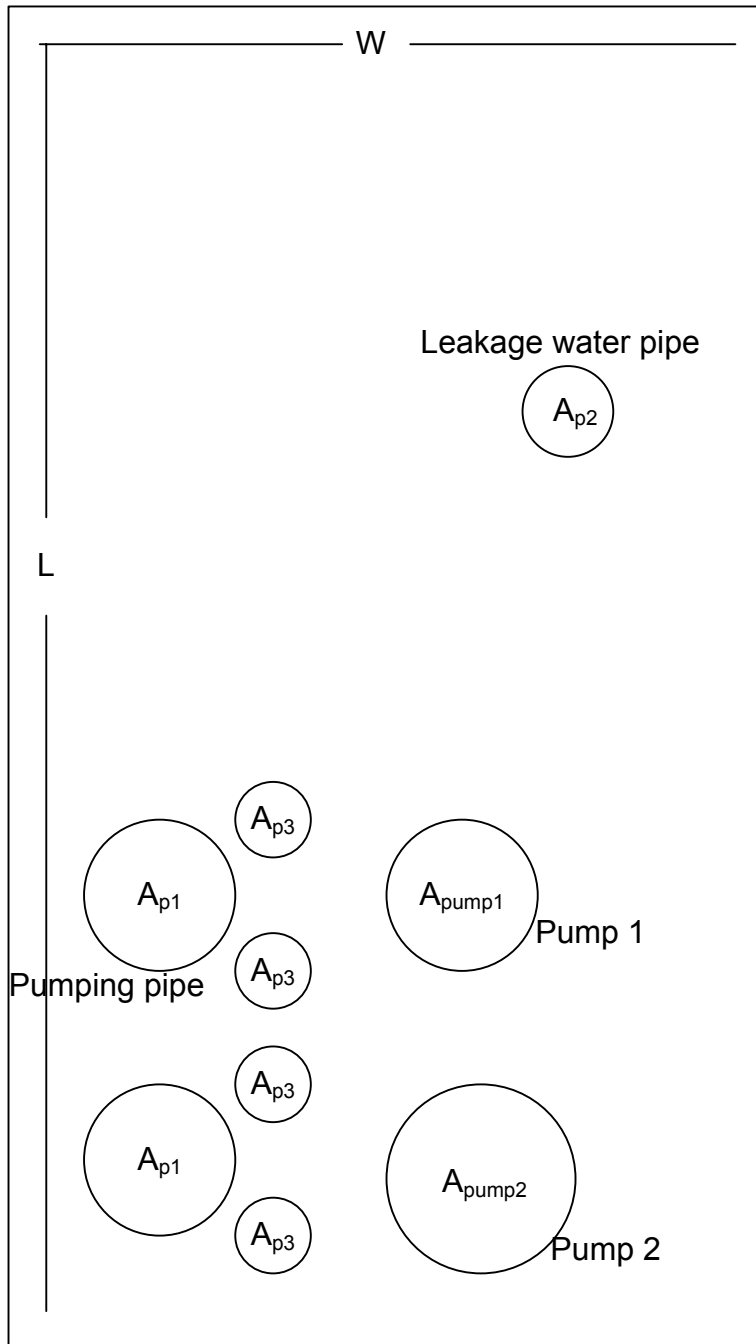
Flow rate turbine inlet	Q_1	m^3/s	50	80	90
Inlet					
Inlet velocity	v_i	m/s	2.2	3.5	3.9
Reynolds number	Re_d	-	5.74E+6	9.18E+6	1.03E+7
Friction factor	f	-	0.013	0.013	0.013
Inlet loss coefficient	K_{inlet}	-	0.500	0.500	0.500
Gate loss coefficient	K_{gate}	-	0.100	0.100	0.100
Diffuser loss coefficient	K_{diff}	-	0.085	0.085	0.085
Friction loss coefficient	$K_{friction}$	-	0.010	0.010	0.010
Sum forebay loss-coefficients	K_{sum}	-	0.695	0.695	0.695
Inlet head loss	h_{inlet}	m	0.17	0.43	0.54
Penstock					
Penstock velocity	v_p	m/s	1.96	3.14	3.53
Friction factor	f	-	0.012	0.012	0.012
Reynolds number	Re_d	-	6.25E+6	9.99E+6	1.12E+7
Friction loss	$K_{friction}$	-	0.079	0.079	0.079
Upper bend loss coefficient	K_{b1}	-	0.130	0.130	0.130
Lower bend loss coefficient	K_{b2}	-	0.110	0.110	0.110
Nozzle loss coefficient	K_{nozz}	-	0.054	0.054	0.054
Sum loss coefficients	K_{sum}	-	0.372	0.372	0.372
Penstock head loss	$h_{penstock}$	m	0.07	0.19	0.24
Total head loss	h	m	0.24	0.61	0.78

Head loss at Vessingfoss.

$$h = 0.000096 * Q^2 [m]$$



The leakage water basin at Vessingfoss;
Measured site dimensions used for calculation of area.



Leakage water basin area			
Basin, length/width	$L \times W$	m^2	9.894
2xPumping pipes	$2 \times A_{p1}$	m^2	0.159
Leakage water pipe	A_{p2}	m^2	0.006
4xSmall pipes	$4 \times A_{p3}$	m^2	0.025
Pump1	A_{pump1}	m^2	0.067
Pump2	A_{pump2}	m^2	0.124
Net area	A_{Q3}	m^2	9.512

```
function [iterback,iterforw,back,forw]=mydiff(func,x1)
% mydiff.m is a simple numerical derivation function implemented in Matlab
% 7.0 which relies on one step forward- and backward differences.
% Programmed by Leif Parr, may 2007
% This function should always be used in conjunction with a graphic
% qualitative evaluation of the function @func.

% func=@matlab_function, a function of one parameter
% x1=value of the parameter in the point of derivation
% iterback=number of iterations in the backward difference
% iterforw=number of iterations in the forward difference
% back=the derivative of @func in x1 by backward difference
% forw=the derivative of @func in x1 by forward difference

% Boolean control parameters
forward=true; % if true, carries out forward difference,
              % if false iterforw=-1, forw=0
backward=true; % if true, carries out backward difference,
              % if false iterback=-1, back=0

% Convergence and step parameters
criteria=1e-10; % iteration stops when the difference between the
              % last and current derivative is less than criteria.
step=99.6; % dx=dx*step/100. The step size dx decreases by step%
          % for each iteration
first_step=0.0001; % [%] dx=x1*first_step/100, value of first stepsize
iter_limit=10000; % if the number of iterations reaches this limit,
                % an error occurs

% backward difference
if ~backward
    back=0;
    iterback=-1;
else

residue=criteria+1;
if (x1==0)
    dx=0.01; % if the derivative is to be evaluated in x1=0, then
            % a nonzero value of dx must be ensured
else
dx=x1*first_step/100;
end
dy_dx=(feval(func,x1)-feval(func,x1-dx))/dx;
iter=0;
while residue>criteria
    dx=dx*step/100;
    dy_dx_new=(feval(func,x1)-feval(func,x1-dx))/dx;
    residue=abs(dy_dx_new-dy_dx);
    dy_dx=dy_dx_new;
    iter=iter+1;
    if iter>iter_limit
        error('Function does not converge.');
```

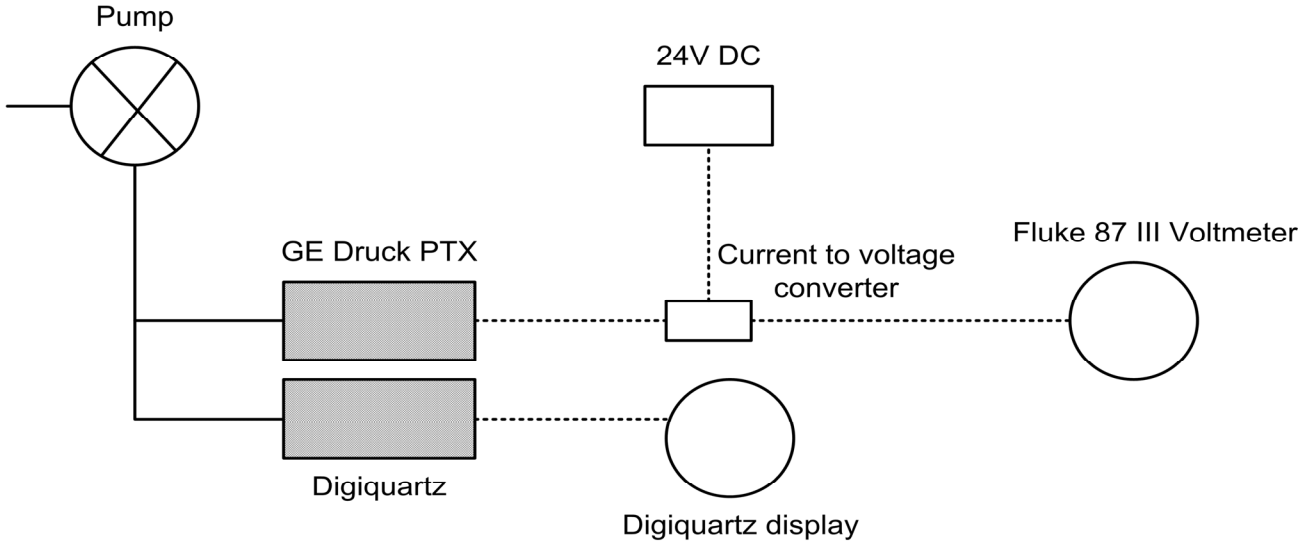
```
end

% forward difference
if ~forward
    forw=0;
    iterforw=-1;
else

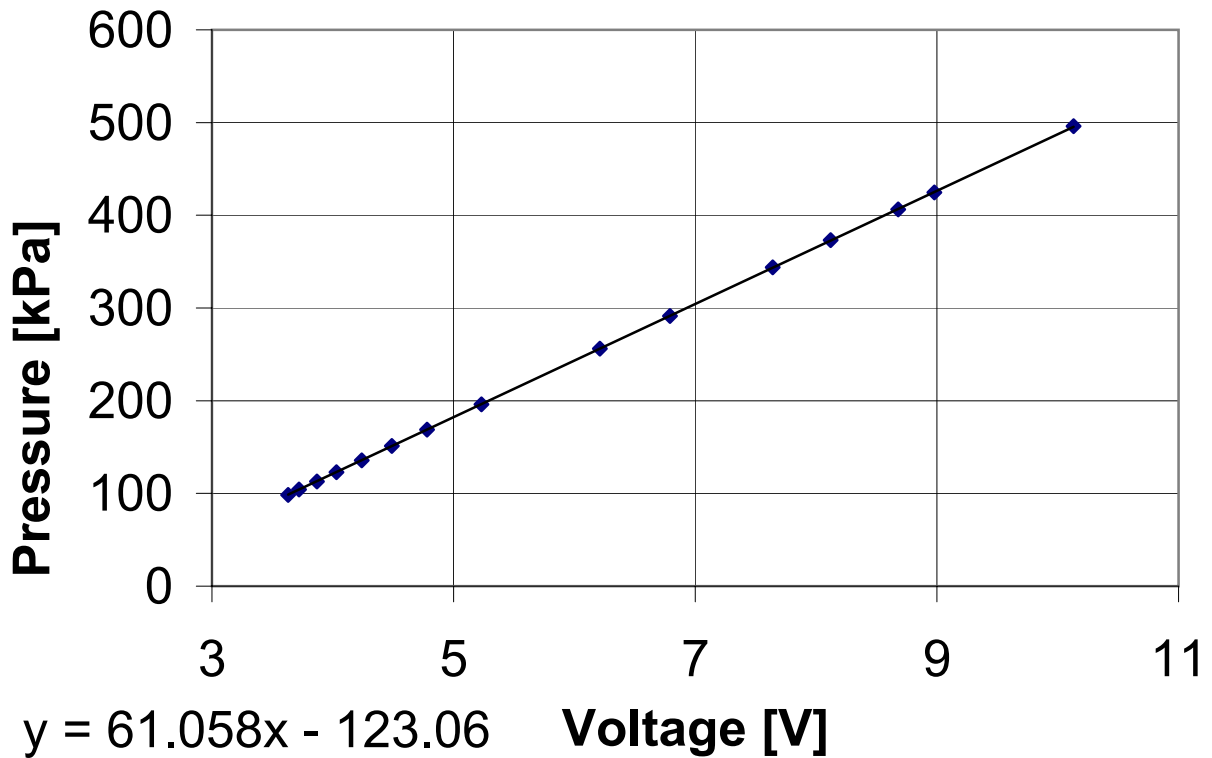
residue=criteria+1;
if (x1==0)
    dx=0.01;
else
dx=x1*first_step/100;
end
dy_dx=(feval(func,x1+dx)-feval(func,x1))/dx;
iter=0;
while residue>criteria
    dx=dx*step/100;
    dy_dx_new=(feval(func,x1+dx)-feval(func,x1))/dx;
    residue=abs(dy_dx_new-dy_dx);
    dy_dx=dy_dx_new;
    iter=iter+1;
    if iter>iter_limit
        error('Function does not converge. ');
    end
end
forw=dy_dx;
iterforw=iter;
end
```

Calibration of tailwater pressure transducer

The calibration was carried out at the Waterpower laboratory NTNU, 15.05.2007 by Leif Parr. The instrumentation setup and result is shown in the figure and graph below.



GE Druck PTX s.n^o 2513105



VANNSTANDSKONTROLL AV MAGASIN OG ELVER

TEV NEAVERKENE

MANUELL KONTROLL, MÅNEDLIG	MÅNED:	April	2007	
----------------------------	--------	-------	------	--

STED	DATO	KL.	VANNSTAND		ISFORHOLD			MERKNAD	
			Manuelt	Inst.	Helt	Delv.	Ikke	Temp.	Vær
Kjeldstadfoss	24.04.07	09.20	172,71	172,71			x	10	Pent
Kulset Bru	24.04.07	?	160,11	160,14			x	10	Pent
Hegset Dam	17.04.07	08:00	253,4	253,42	X			1	Pent
Gresslifoss	16.04.07	10:45	288,48	288,49			X	12	Lettskyet, opphold
Aune	16.04.07	12:15	292,31	292,3			X	12	Lettskyet, opphold
Finnkoisjø	25.04.07	11.00	761,91	761,91	X			1	Pent stille
Gammelv.sjø	25.04.07	10.00	502,2	502,21	X			5	Pent stille
Sellisjø									
Håene	16.04.07	09:55	528,55	528,61		X		10	Lettskyet, opphold
Stugusjø	24.04.07	13.00	599,92	599,94	X			7	Pent
Vessingsjø	17.04.07	10.30	670,27	670,27	X			10	Pent
Nesjø	19.04.07	12:00	723,74	723,75	X			0	Snøbyger
Falksjø									
Sylsjø	19.04.07	12.00	835,32	XXX	X			3	Pent

NB: I merknadsrubrikken Vær; noteres pent,overskyet, regn/snø.

STED	DATO	KL.	VANNSTAND		ISFORHOLD			MERKNAD	
			Manuelt	Inst.	Helt	Delv.	Ikke	Temp.	Vær
Kjeldstadfoss									
Kulset Bru									
Hegset Dam									
Gresslifoss									
Aune									
Finnkoisjø									
Gammelv.sjø									
Sellisjø									
Håene									
Stugusjø									
Vessingsjø									
Nesjø									
Falksjø									
Sylsjø									

NB: I merknadsrubrikken Vær; noteres pent,overskyet, regn/snø.

Sendt 26/4 - 07

Zyön G